Aaro Tuisku

Wavelength Dispersive X-ray Fluorescence Method Development for Asphaltene Samples

Metropolia University of Applied Sciences

Bachelor of Laboratory Services

Laboratory Sciences

Bachelor´s Thesis

4.2.2018

Author	Aaro Tuisku
Title	Wavelength Dispersive X-ray Fluorescence Method Development for Asphaltene Samples
Number of Pages	45 pages + 1 appendix
Date	4 February 2018

Degree	Bachelor of Laboratory Services

Degree Programme	Laboratory Sciences

Instructors	Michaela Banzhaf, XRF specialist
	Mia Ruismäki, Senior Lecturer

This study was carried out at Neste Research and Development unit in Porvoo. The aim was to develop a specialised quantitative method for asphaltene samples with wavelength dispersive X-ray fluorescence (WDXRF). Prior to this work the samples were analysed with a semi-quantitative WDXRF method and improvements in accuracy were wanted especially for the lower concentration range (0-100 ppm).

Over twenty elements are measured from the asphaltene samples with WDXRF but for this work twelve elements were included: potassium, calcium, chromium, manganese, cobalt, copper, zinc, cadmium, tin, antimony, thallium and lead.

XRF is a non-destructive analytical method, where the matrix has a strong influence to the received results. Samples are measured as undiluted with minimal sample preparation and high sensitivity is gained. WDXRF allows to optimise the measuring parameters for each analyte individually and high resolution can be obtained.

In this work reliable and reproducible calibration sample preparation was accomplished with pipetting various concentrations of element standards into ethanol and mixing a representative blank sample into it. The calibration samples were air-dried in a fume hood and pressed as pellets afterwards. Linear spiking concentrations were obtained.

For each measured element the measuring conditions were optimized: Different X-ray tube settings, primary filters, analysing crystals and collimators were tested with quick (~3 min) qualitative analyses. Background positions and pulse height analyser windows were set in the quantitative method. The calibration curves were measured and corrections were applied if needed, and high accuracy curves were achieved (RSD <0.0001-0.0006%). Longevity of the method was ensured with suitable drift samples.

The method development produced a quantitative WDXRF method for asphaltene samples which can now be further tested and validated. The study also gained the laboratory knowledge for expanding the rest of the analysed elements under a quantitative WDXRF method as well.

Keywords	XRF, WDXRF, method development, asphaltene

Tekijä Otsikko Sivumäärä Aika	Aaro Tuisku Menetelmänkehitys asfalteeninäytteille aallonpituusdispersiivisellä röntgenfluoresenssispektrometrialla 45 sivua + 1 liite 4.2.2018
Tutkinto	Laboratorioanalyytikko (AMK)
Koulutusohjelma	Laboratorioala
Ohjaajat	XRF-asiantuntija Michaela Banzhaf Lehtori Mia Ruismäki

Opinnäytetyö suoritettiin Nesteen Tutkimus- ja kehitysyksikössä Porvoon jalostamolla. Työn tarkoituksena oli kehittää kvantitatiivinen menetelmä asfalteeninäytteille aallonpituusdispersiivisellä röntgenfluoresenssispektrometrialla (WDXRF). Työn tavoitteena oli kehittää näytematriisille tarkka menetelmä, joka keskittyisi mataliin pitoisuuksiin (0-100 ppm). Ennen tätä työtä asfalteeninäytteet oli mitattu puolikvantitatiivisella menetelmällä.

Asfalteeneista mitataan WDXRF:lla yli 20 alkuainetta, mutta tämän työn menetelmään sisällytettiin 12 alkuainetta kohtuullisen työmäärän saavuttamiseksi: kalium, kalsium, kromi, mangaani, koboltti, kupari, sinkki, kadmium, tina, antimoni, tallium ja lyijy.

Röntgenfluoresenssispektrometriassa näytettä ei hajoteta ja näytematriisilla on suuri vaikutus saatuihin tuloksiin, mutta korkea sensitiivisyys saavutetaan. Näytteet voidaan mitata laimentamattomina ja näytteiden esikäsittely on yksinkertaista ja nopeaa. WDXRF:n optiikka mahdollistaa korkean resoluution sekä jokaisen mitattavan alkuaineen erillisen optimoinnin.

Menetelmän kehitys aloitettiin oikeellisten ja toistettavien kalibrointinäytteiden valmistamisesta. Toimiva lineaarinen standardin lisäysmenetelmä saavutettiin pipetoimalla alkuainestandardeja eri pitoisuuksissa etanoliin, johon nolla-näyte sekoitettiin. Kalibrointinäytteiden annettiin kuivua vetokaapissa ja näytteet painettiin puristenapeiksi analysointia varten.

Jokaiselle kalibroitavalle alkuaineelle optimoitiin mittausparametrit kokeilemalla eri röntgenputkiasetuksia, suodattimia, analyysikristalleja ja kollimaattoreja lyhyillä (~3 min) kvalitatiivisilla mittauksilla. Kvantitatiivisessa menetelmässä mittauspisteille määritettiin taustapisteet sekä sopiva pulssi-ikkuna. Mitatut kalibrointisuorat noudattivat korkeaa tarkkuutta (RSD <0,0001-0,0006 %). Kalibroinnin jälkeen kalibrointisuorille mitattiin referenssi-intensiteetit drift-näytteillä menetelmän ylläpidon mahdollistamiseksi.

Työn tuloksena onnistuttiin kehittämään kvantitatiivinen WDXRF-menetelmä asfalteeninäytteille validointia ja käyttöönottoa varten. Menetelmän kehitys antoi laboratoriolle mallin siirtää loputkin WDXRF:lla analysoitavat alkuaineet uudelle kvantitatiiviselle menetelmälle.

Avainsanat	XRF, WDXRF, menetelmänkehitys, asfalteeni

Metropolia

Contents

Metropolia

Abbreviations

XRF   X-ray fluorescence. Analytical method which analyses characteristic X-ray radiation from a sample generated by an external X-ray source.

WDXRF   Wavelength dispersive X-ray fluorescence. XRF analysis method.

EDXRF   Energy dispersive X-ray fluorescence. XRF analysis method.

PHA   Pulse height analyser. XRF energy distribution analyser.

FP   Fundamental parameters method. XRF quantitative method.

SDA   Solvent deasphalting. An industrial separation process.

ppm   Parts per million. Relative unit.

1 Introduction

This study was conducted at X-ray fluorescence laboratory in Neste Research and Development unit in Porvoo. The aim was to develop an optimized quantitative wavelength dispersive X-ray fluorescence (WDXRF) method for asphaltene samples. Prior to this work the samples have been analysed with a semi-quantitative WDXRF method. The new method was created to produce accurate results at low ppm-range (0-100 ppm). XRF is an interactive analysing method where the sample matrix have a strong influence to the received results. In XRF, the sample is not decomposed which can complicate the method development but the sample preparation is most often quick and easy. Also the analysing times stay rather low and high sensitivity is achieved. [1]

In 2017 Solvent Deasphalting (SDA) unit was established in Porvoo refinery to supplement Production Line 4, the diesel production line. In the SDA-unit asphaltene is removed from the oil to increase the distillation yields and the production line usability since asphaltene is a very dirtying component in oil. [2] [3] [4]

The asphaltene samples are sent to the laboratory monthly and full elemental composition of the samples are analysed. The composition is important to know for its further use. For example, the asphaltene can be used as raw material in power plant of Porvoo to produce steam and electricity. Among asphaltene samples also vegetable oils, animal fat, catalysts and fuels are being analysed in the laboratory by XRF. [5]

Neste Oyj is an oil refining and marketing company that produces oil and renewable products for transports, businesses and consumers. Neste was established in 1948 to produce and ensure the oil production in Finland. Today Neste is a global company that has oil refineries in Porvoo, Naantali, Rotterdam and Singapore. Neste highly supports ecological solutions and is the world´s biggest producer of renewable fuels. Porvoo refinery is focused on premium-quality fuels and includes four production lines that produce in total 12 million tons of petroleum annually. [2] [6]

2 Asphaltenes

Solvent deasphalting is a process where asphaltenes are separated from oil by molecular weight. Asphaltenes are precipated by paraffinic solvents and removed. Products of solvent deasphalting are low-contaminant deasphalted oil (DAO) and the contaminant residue, asphaltenes. In Porvoo the removed asphaltene is stored mainly as solid pellets (Figure 1, left). [4] [7]

Figure 1. Solid asphaltene (left) and the hypothetic chemical composition of asphaltene (right). [8] [3]

Asphaltenes are found in crude oil and bitumen as fractions and are defined by their solubility (to a certain paraffin). They are soluble in aromatic solvents such as toluene and benzene but precipitate in n-alkanes such as n-pentane, n-hexane, n-heptane etc. Asphaltenes tend to form aggregates which lead to clusters and precipitation. Asphaltenes precipitate in oil production due to multiple phases of heating, cooling, high pressures, mixing with other oils and fragment separations and are typically separated as components that do not dissolve into heptane or pentane but dissolve into toluene. [3] [9]

Asphaltenes have complex structures (Figure 1, right) and are the heaviest and the most aromatic component in oil with molecular masses of approximately 700-1000 u. Elemental composition of asphaltenes is mostly comprised of carbon, hydrogen, nitrogen, oxygen and sulphur. For example, N-pentane precipitated asphaltenes often have mass percentages of 80-85% of carbon, 7-10% of hydrogen, up to 10% of sulphur, 5% of oxygen, 3% of nitrogen and trace amounts of vanadium and nickel. [3]

3   Wavelength Dispersive X-Ray Fluorescence Analysis (WDXRF)

3.1   X-ray Fluorescence Analysis

X-rays were discovered in 1895 by Wilhelm Röntgen and in the early 1950s fluorescence approach got its first commercial instrumentations. Wavelength dispersive spectrometers became to public use in the late 1960s and today it is one of the most used methods for elemental composition of a sample, for both qualitative and quantitative determination. XRF brings advantages such as minor requirements for sample preparation, non-destructive analysis platform, relatively short analysis runtime, wide elemental analysis range from Be to U and linearity from ppm to 100%. [10] In XRF-analysis two groups of spectrometer configurations are most commonly used: Wavelength Dispersive (WD)XRF- and Energy Dispersive (ED)XRF spectrometers. In WDXRF the fluorescent X-rays are physically separated before detection using diffraction crystals when in EDXRF the fluorescent X-rays are measured simultaneously and separated in solid-state detector. WDXRF offers excellent signal-to-noise ratio and peak separation leading to very low background noise and high resolution. Mechanically more complicated WDXRF spectrometers have many moving parts and usually more power and are thus often more expensive than EDXRF-spectrometers. [11]

3.2   Introduction to X-Rays

X-rays are electromagnetic radiation with wavelength region from 0.01 nm to 10 nm (100 keV-0.1 keV). X-rays are composed of photons, just like all electromagnetic radiation from short radioactive gamma-rays to long radio waves (Figure 2).
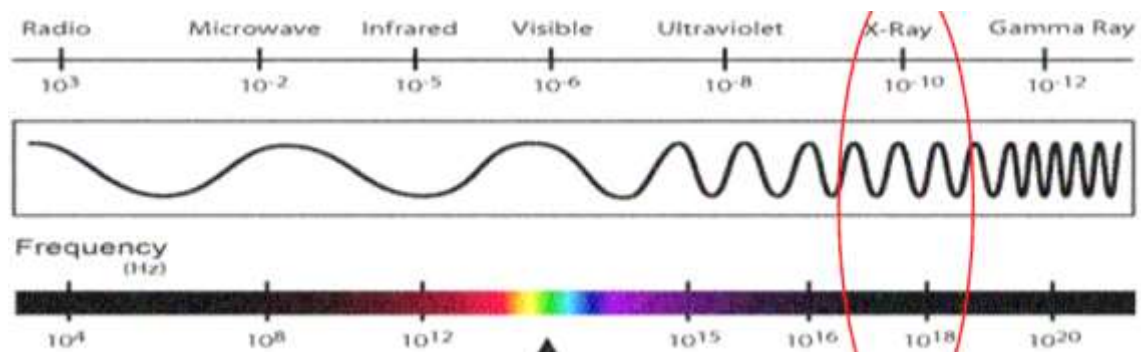

Figure 2. The spectrum of electromagnetic radiation. [3]

Photons have a dual character: They have the properties of both waves and particles. A photon is diffracted if set through a crystal which proves the characteristics of waves. A photon also has energy and can collide and interact with other particles which, in turn, depicts the characteristics of particles. [12] Because of the dual characteristics, photons can be thought of as particles moving like a wave (Figure 3). The dual characteristics make the WDXRF optical path possible and is therefore crucial to the analysis. [10]
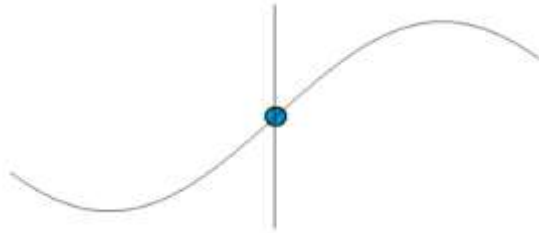

Figure 3. X-Rays are particles moving like a wave. [3]

The energy of a photon is related to its wavelength and is explained with the Duane-Hunt equation (equation 1):

$$E = hv = \frac{hc}{\lambda} = \frac{1.24}{\lambda}, \text{ where} \tag{1}$$

E = energy (eV)
h = Planck constant (4.14 x 10^{-15} eV*s)
v = photon frequency
c = speed of light (3.00 x 10^8 m/s)
λ = photon wavelength (nm).

The Duane-Hunt equation shows that a photon´s wavelength is inversely proportional to its energy: long wavelength equals low energy and short wavelength equals high energy. X-rays have short wavelengths and thus high energy. The high energy is enough to ionize atoms by removing electrons from their orbitals which creates ions. Because of the ionization abilities X-rays are also called as ionising radiation. [11] [12] [13]

3.3   XRF Safety

Ionising radiation, such as X-rays, might cause cancer and genetic defects if exposed to. Although in XRF the X-rays have rather low energy, the intensities can be quite high. However, the current XRF spectrometers are very safe. The spectrometers are built to

prevent the harmful levels of X-rays from escaping outside the spectrometer. The X-ray tube only produces X-rays when the tube is turned on and the samples do not become radioactive after the analyses. The legal exposure limits to X-rays are determined by law. Earlier X-ray dosimeters and other safety equipment were mandatory around XRF spectrometers but today most countries have dismissed the legislation because of the high safety levels of the modern day XRF spectrometers. [1]

3.4   X-ray Fluorescence

X-ray fluorescence is the key element in XRF measurements. X-ray fluorescence is produced by transitions of inner shell electrons of an atom which results the atom to emit X-ray photons with a characteristic wavelength determined by the atomic number of the element. The fluorescent radiation from a sample can be generated by emitting external X-ray radiation into the sample, referred to as primary radiation. The primary radiation can eject an inner shell electron of an atom in the sample, if a primary photon energy is equal or higher than the binding energy of the electron, which will create an unstable intermediate ion. To fix the inner shell electron deficit, an outer shell electron moves to the created empty gap. In the electron transition energy is released as fluorescence radiation which energy is equal to the energy difference between the electron shells.

The energies that release the electrons from the energy shells are determined by the atomic number of the element, which makes the fluorescence characteristic. Elements with lower atomic number require less energy and are referred to as light elements. Higher atomic number elements have shorter wavelengths and require more energy and are referred to as heavy elements. The X-ray fluorescence is illustrated below in Figure 4. [14] [11] [15]
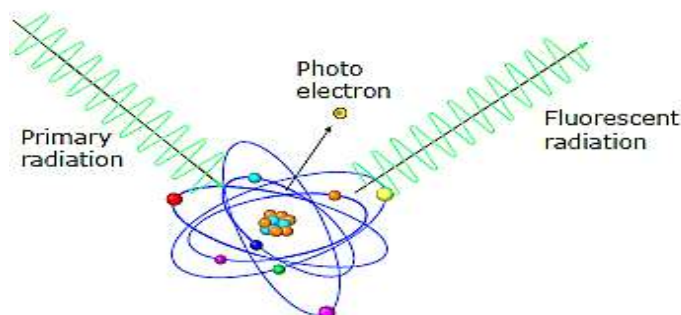

Figure 4. XRF- radiation [10]

Electrons travel within shells surrounding a positively charged nucleus. Bohr´s atomic model, shown below in Figure 5, is used to describe the different energy shells and their sub-levels.
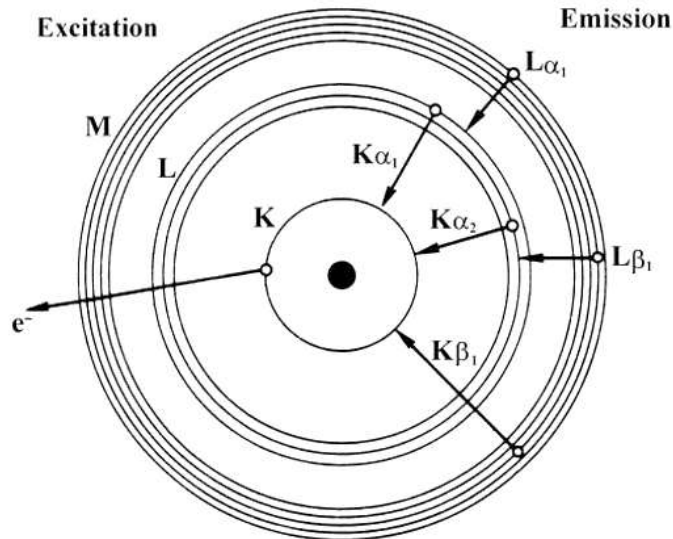

Figure 5. Bohr´s atomic model [10]

The shells are named K, L, M, N, etc. The K-shell is the innermost shell and takes two electrons. The L-shell consists of three sub-levels and contains up to eight electrons. The M-shell consists of five sub-levels and contains up to eighteen electrons. [14] Different fluorescent radiations are named by their electron transitions. First the location of the ejected electron is described. For example, when a K-shell electron has been ejected and an outer shell electron replenishes the empty gap the fluorescence is called K-radiation. Then the starting point of the electron from the outer shell is described with the Greek letters. A (alpha) indicates a single jump between the shells (for example from L-shell to K-shell) and β (beta) a two shell jump (for example from M-shell to K-shell). In sub-level changes numbering is used (1,2,3 etc.). Therefore, if an electron from sub-level 3 on L-shell would replenish an ejected electron from the K-shell, the fluorescent radiation would be called $K\alpha_1$, or alternatively KA1 in a simplified spelling. [14]

3.5   Instrument Principle and Parameters

WDXRF-analysis is based on the sample excitation by X-rays and the detection of the characteristic X-rays. The X-ray source, the tube, creates the X-ray beam. Before the X-ray beam penetrates the sample, it can be filtered if desired. The X-ray beam from the tube is referred to as primary radiation and the X-rays emitted by the sample as secondary X-rays. The secondary X-rays are collected by the collimator and directed to the analysing crystal which together determine the spectral resolution in WDXRF. After analysing crystal the X-rays go to the detector and to the pulse height analyser to be measured. Below in Figure 6 the optical path of WDXRF is illustrated.
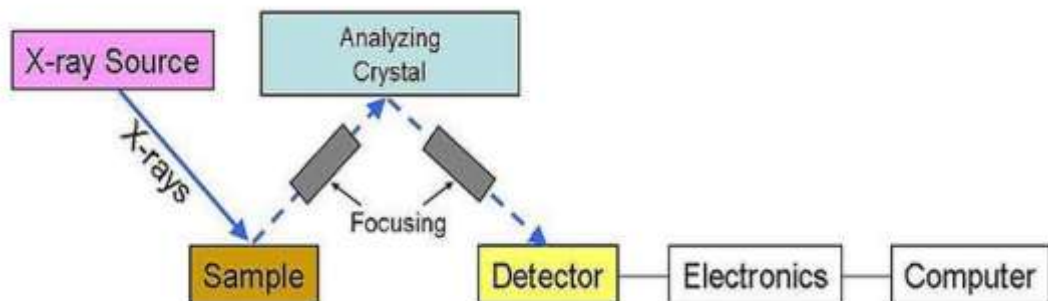

Figure 6. The optical path in WDXRF. The X-ray source and the optics can either be above the sample like in this picture or vice versa. [10]

The instrument used in this work had a special feature of a tube-above configuration where the X-ray tube and the optics are placed above the measured sample (as in Figure 6). The other configuration would be the other way around, tube below configuration. Placing the tube and the optics above the sample eliminates contamination falling from analysed samples but may not be as practical for liquid and powder samples, as the sample is turned upside down during the analysis. [16]

3.5.1   X-ray Tube

The purpose of the X-ray tube is to generate the primary X-ray beam. Since every element have different excitation energies, the X-ray tube needs to provide a stable, high-intensity X-ray beam with a wide range of energies for efficient sample excitation.

There are a few different tube types, the end-window and side-window types being the most typical ones. However, all the X-ray tubes work on the same principle utilizing an electrical field for electron acceleration and suitable anode material for deceleration. The XRF-spectrometer used in this work was equipped with the end-window model which is also the most common type and therefore is introduced. [1]

Characteristics for the end-window tubes (Figure 7) are that the anode has a high positive voltage and the beryllium exit window is at the front end of the housing. In the end-window tube the filament, negative potential cathode, is set around the positive potential target anode in a ring. The filament is set to zero voltage and is heated by direct current to cause a negative potential and produce "free" electrons. Potential difference increases between the negative filament and positive target and the electrons start to accelerate across the potential difference gaining kinetic energy. Electrons are decelerated by the atoms of the positive target and the kinetic energy of electrons is transferred to the atoms. Excessive energy in the anode atoms results into fluorescence, generating the X-rays. [17] [10]
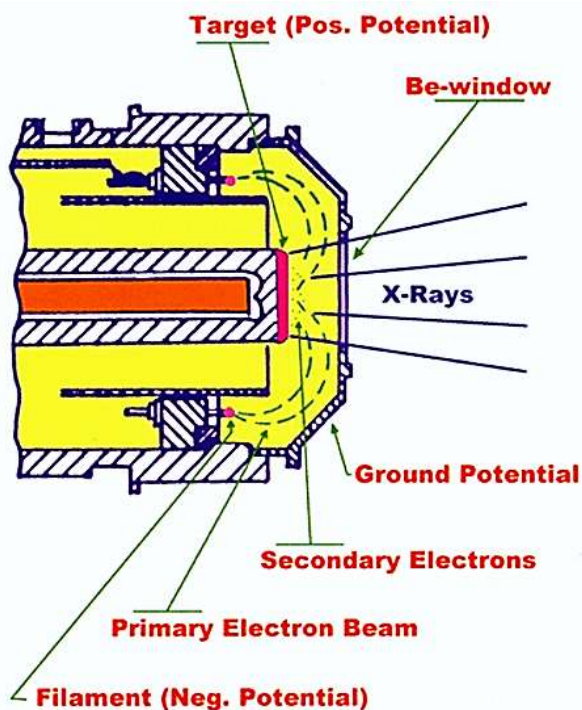

Figure 7. The end-window X-ray tube configuration. [10]

The end-window tube provides versatile measurements but lack the higher kV range (+60 kV) which is required in K-line analysis of heavy elements. The alternative window type side-window tube is more powerful (100 kV), which allows the K-line measurements

of heavy elements. As a downside, its thicker beryllium window restricts the use of weaker long wavelength L-lines in measurements. [14] [1]

3.5.2 Excitation Condition

The sample excitation is based on the excitation condition which consists of the applied voltage and the current in the tube. Also the created excitation beam can be filtered with primary filters if beneficial. [18]

3.5.3 Tube Voltage and Current

Tube voltage is the positive charge (kV) of the target and the tube current (mA) is the electron flow from the heated filament to the target. Both of them are adjustable parameters. The total voltage and current applied regulate the overall measuring intensity. More powerful continuous X-ray is produced when the applied voltage and current is increased. To detect a specific element, efficient amount of X-ray energy is needed but excessive energy does not change the excitation effect for the specific element, but may negatively affect the peak resolution. Generally, high voltage is recommended to be used with heavy elements and high current with light elements (Table 1). [10]

Table 1. Guideline voltages for different elements by Rigaku. [9]

Applied Voltage	Element for measurement of K line	Element for measurement of L line
30kV	Be - Cl	
40kV	K, Ca	
50kV	Sc - Ba	Ba - U

In this work higher (+10 kV) voltages were used. Guidelines change by the used application and between source materials. [1]

3.5.4 Target Material

The target material of the X-ray tube affects the excitation as well. Typically an XRF spectrometer is equipped with one X-ray tube with one selected target material but some special XRF spectrometers have dual target X-ray tubes which have two targets in one

X-ray tube. For the target materials most common alternatives (Figure 8) are rhodium (Rh), chromium (Cr) and tungsten (W).
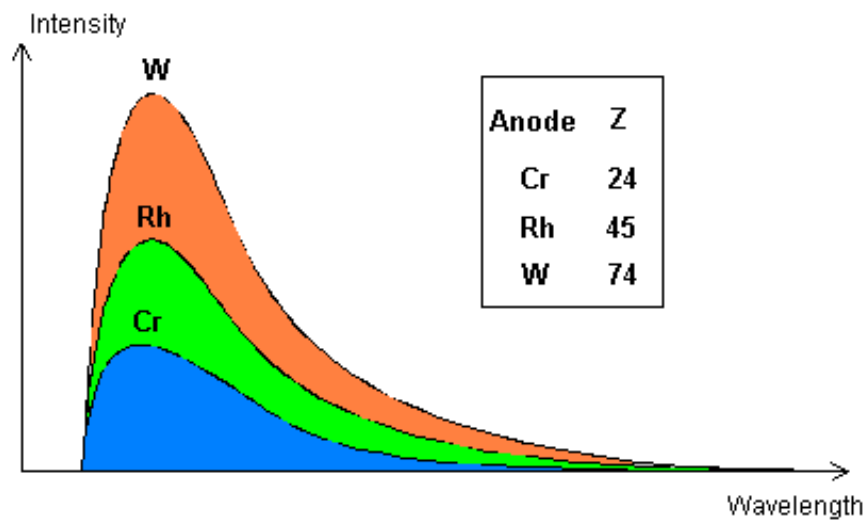

Figure 8. Influence of the anode target material of the tube. Higher Z gives higher intensity primary X-rays. [17]

Rhodium is the most all-round target material and is effective for all XRF measurable elements (Be - U), chromium target is effective for Ti - Cl (~light elements) and tungsten target for rare-earth elements (~heavy elements). The spectrometer used in this work had a rhodium target anode. [18] [1]

3.5.5   Bremsspectrum

The X-ray tube distributes simultaneously the full range of the needed energies, referred as Bremsspectrium, which produces the desired characteristic X-rays from the sample. However, part of the Bremsspectrum can be scattered from the surface of the sample and reach the detector creating background. While most part a continuous background is produced, the characteristic element lines of the anode material and its scattering usually produces a major background peaks (Figure 9). [14]
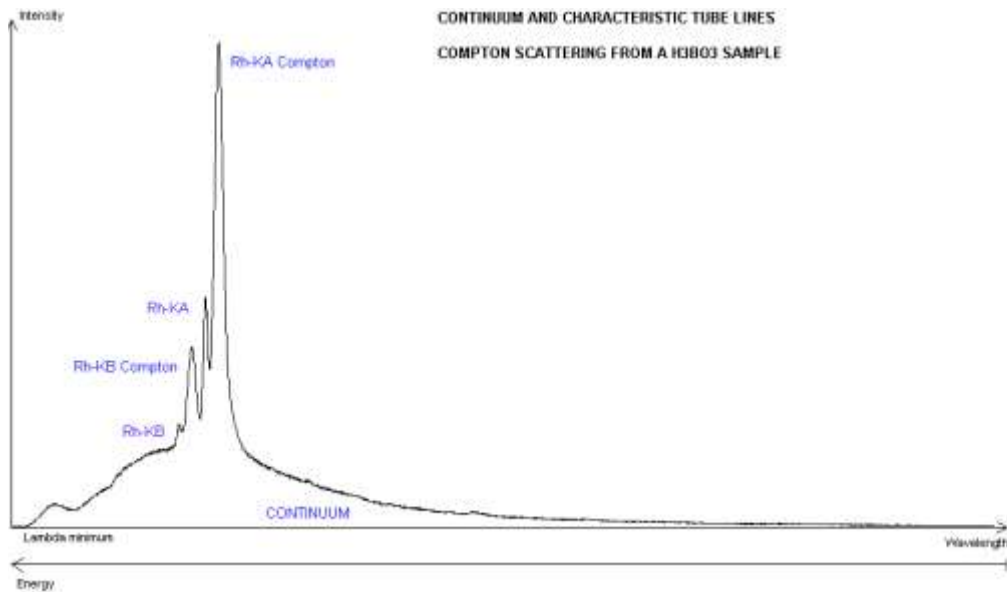
Figure 9. The Bremsspectrum of a rhodium X-ray tube including the Compton ad Rayleigh scattering. [12]

Two types of scattering may happen: Rayleigh and Compton scattering. In Rayleigh scattering the anode photons (rhodium in this case) are scattered from the sample directly to the detector without losing energy creating the characteristic elemental lines of Rh-KA and Rh-KB. If rhodium or other close element is the measured element, a filter can be used to absorb the elemental line before it hits the sample. In Compton scattering the anode photons collide with the electrons of the sample and loose energy before scattering to the detector. The scattering intensities vary between different samples and depend on the sample matrix. The scattering is more intensive with samples that consist of lighter elements than with samples that consist of heavier elements. [14]

3.5.6   Primary Filters

The primary beam from the tube can be modified by using primary filters. The primary filters are placed between the X-ray tube and the sample and their purpose is to reduce or eliminate disturbances of the Bremsspectrum.

Continuous X-rays from the tube can be reduced with Ni40 and Al125 primary filters which improve peak-to-background ratio and, thus, are very useful in trace element analyses. Ni40 reduces continuum at moderate energies and is especially effective for Pb L-line and As K-line and was used for Pb L-line in this work. Al125 reduces continuum at lower energies and is especially effective for Ti, Cr and Fe.

Characteristic X-rays from the tube can be absorbed with Ni400 and Al25 primary filters which allow proper detection for element lines overlapped with characteristic peaks of the target of the tube. Ni400 is the heaviest primary filter and it absorbs the K-lines from the X-ray tube but allows very high energy continuum pass through. Ni400 is effective when analysing K-lines of Ru, Rh, Pd, Ag, Cd and other close lines. Al25 in turn absorbs the L-lines of the tube but allows higher energy continuum pass through. It is used in L-line analyses and very beneficial in thin samples analyses. [11] [10]

3.5.7   Collimator

The optic sensitivity and resolution are determined mainly in WDXRF by the chosen combination of collimator and analysing crystal. The secondary X-rays are scattered in all directions from the sample and the purpose of the collimator is to deliver the second-ary X-rays from the sample reliably to the analysing crystal. Collimator consists of parallel soller slits. The soller slits are a set of metal plates which the secondary X-rays are set to travel through. Spacing between the plates affects the sensitivity and the resolution. The less space there is between the plates, the less secondary X-rays will make the way through but higher resolution is gained. The soller slit spacing is presented as the diver-gence of degrees allowed to pass through the slits (Figure 10). [11] [10] [17]
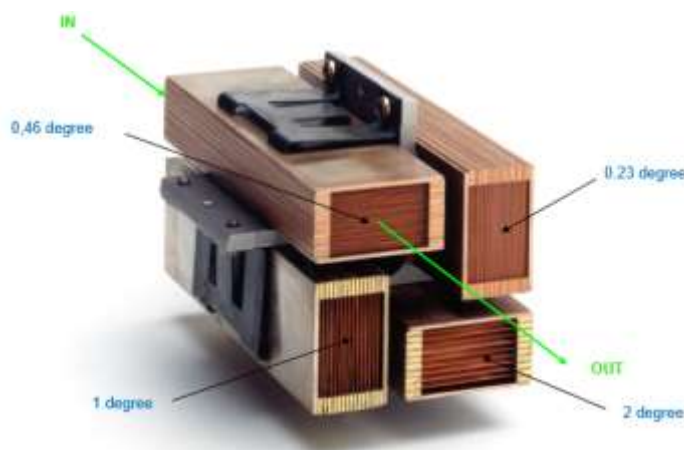

Figure 10. Bruker S4/S8 collimator with 0.23, 0.46, 1 and 2 degree collimator apertures. [17]

In general, lower degree (high resolution) collimators are used with heavy elements and in complex matrixes and higher degree collimators with light elements. [17]

3.5.8 Analysing Crystal

The crystal separates the wavelengths by diffraction and directs them to the detector. When the X-rays come to the crystal, the beam is polychromatic meaning it has all the different wavelengths together. The crystal separates the X-rays by the Bragg´s Law (equation 2) into individual monochromatic light-beams:

$$n\lambda = 2d \sin\theta, \text{ where} \tag{2}$$

n = reflection order (1, 2, 3 etc.)

λ = photon´s wavelenght (nm)

d = distance of the lattice spacing of the crystal (nm)

θ = diffraction angle (θ).

The crystal consists of crystal lattice which consists of sets of parallel atom planes (Figure 11). In the Bragg´s Law the distance between the atom planes is referred as "d" and it determines the angular separation between peaks, the resolution being inversely proportional to the distance. For example, the two crystals used in this work, LiF(200) and LiF(220), had the "d" values of 0.2014 nm and 0.1424 nm, respectively. [1] [17] [14] [11]
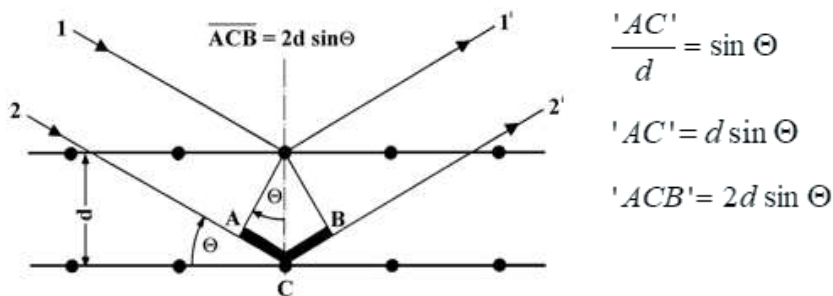

$$\frac{'AC'}{d} = \sin\Theta$$

$$'AC' = d \sin\Theta$$

$$'ACB' = 2d \sin\Theta$$

Figure 11. Bragg´s Law applied to the analysing crystal. [17]

The Bragg´s Law can be fulfilled with multiple reflection orders ("n") as long as the same angle θ is obtained, leading to multiple peaks from one element. So called higher order peaks are produced when the X-rays penetrate through the first layer (n = 1) of the crystal planes to the latter ones (n >1), also seen in Figure 11. Higher order peaks have typically approximately one third of the previous order peak intensity. Up to three orders can be observed if the concentrations are high enough, in theory up to four. Higher order peaks can be excluded in the pulse height analyser (Figure 12). [1] [17]
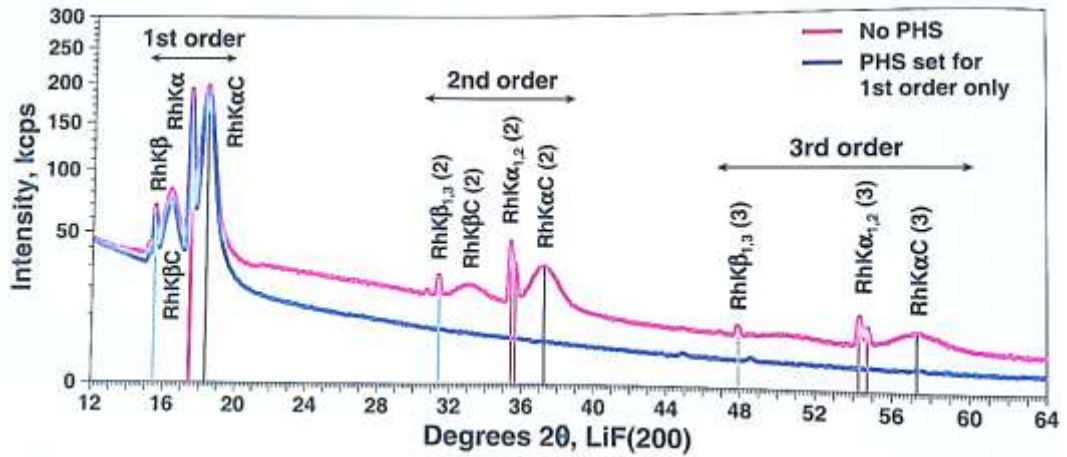
Figure 12. 1st, 2nd and 3rd order peaks of scattered Rh tube peaks when PHA window is set to 50-500% and unaffected straight line when the PHA window is set to 100-300%. [1]

In WDXRF spectrometers there are different crystals used to choose for. Two main qualities of the crystal are its reflection ability which affects the peak intensities and the crystal d-spacing (Figure 11) which affects the resolution. The reflectivity is usually proportional to the d-spacing. [1] Optimal crystal choice is determined by the wavelength of the element and generally crystals with longer d-spacing are used with light elements and crystals with shorter d-spacing are used with heavier elements. Below in Figure 13 recommended crystal choices by Rigaku [10] are listed.

Figure 13. Crystal choice table by Rigaku. LiF(200) has the shortest d-spacing (0.2014 nm) and RX75 has the longest d-spacing (~20 nm). [10] [17] [1]

3.5.9   Detector

An X-ray detector converts X-ray photons coming from the crystals into a measurable energy form, voltage pulses. Because the full range of X-ray wavelengths is rather wide, 0.012-12 nm (100-0.1 keV), two different detectors are used: gas proportional counter and scintillation counter detector (Table 2). [18]

Table 2. Detector types in WDXRF. [13] [14]

Detector type	Wavelength/energy coverage	Suitable for
Gas proportional counter	0.08 - 12nm / 15-0.1 keV	Light elements (Be-Cr)
Scintillitaion counter	0.012 - 1.5nm / 100-8keV	Heavy elements (Mn-U)

Gas Proportional Counter Detector

The gas proportional counter detector utilizes a metallic cylinder filled with inert counting gas and quench gas, most often argon and methane are used, respectively. Inside the cathode cylinder, a thin counter wire anode is set co-axial and a positive high voltage is applied (1400-2000 V). The cylinder also has a sealed entrance window made of material permeable to X-ray photons and thus allowing X-ray photons to enter while keeping the counting gas inside. The detector structure is seen below in Figure 14.
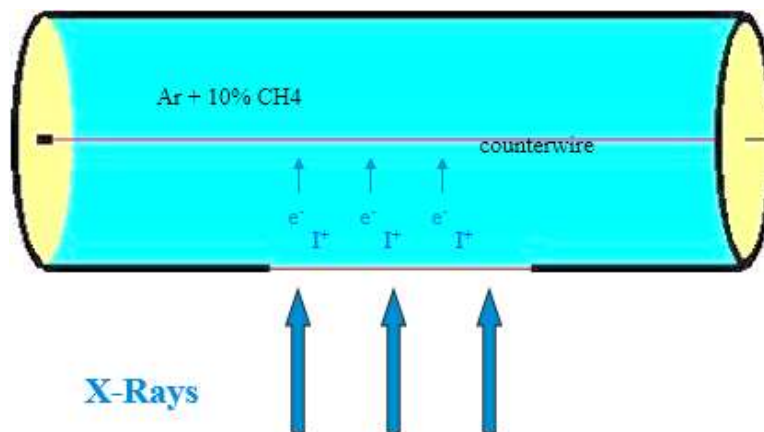
Figure 14. Gas proportional detector [17]

After entering the detector the X-ray photon ionises atoms and molecules of the counting gas. The positively charged counter wire attracts the electrons formed from the ionization to the co-axis and the positive ions to the sides of the cathode cylinder. On the way towards the co-axis an electron ionises more electrons which causes an electron cluster, gas amplification, that when reaching the wire, leads to electric current and a brief decline

in voltage, a pulse. The cylinder is connected to an amplifier where the pulse is registered. The gas atoms are re-formed again with free electrons and with the assist of the quench gas (CH_4). [17]

The gas amplification allows a small quantity of electrons to be amplified significantly and, thus, can be made distinguished from the electronic "noise". [14] But as a downside the incoming X-ray photons may also excite the argon (counting) gas which leads to Ar-KA fluorescence, an escape-peak. [17]

Scintillation Counter Detector

Scintillation counter detector is for detecting heavy elements. Since the low wavelength radiation contains too much energy to be absorbed into the counting gas of a gas proportional detector, light is used to convert X-rays into electric signal. The scintillation counter detector consists of the NaI-crystal, the photo cathode, multiple dynodes and an anode. The structure of the scintillation detector is shown below in Figure 15.
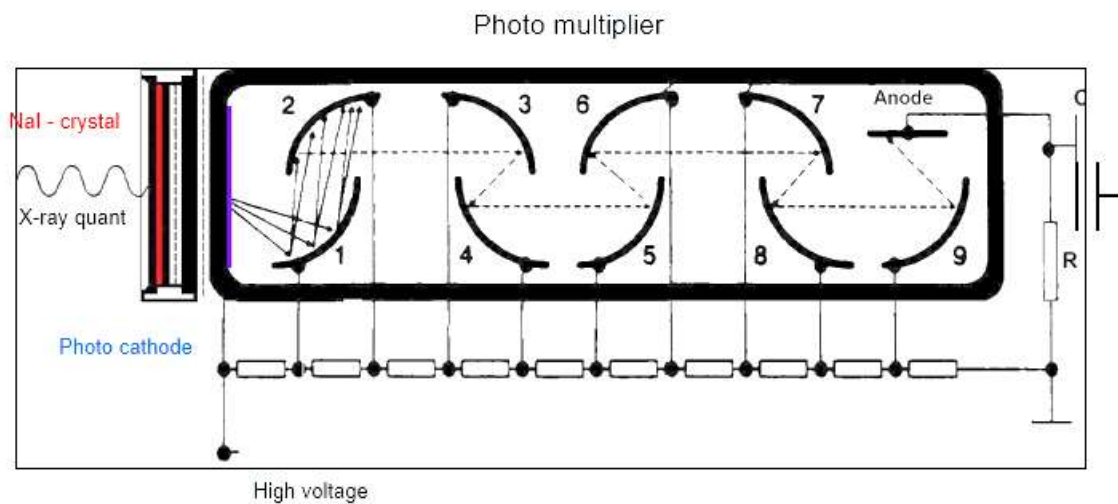
Figure 15. The scintillation counter. [17]

In the scintillation counter the incoming X-ray photons are first converted into flash of blue light (around 410 nm) by thallium activated sodium iodide-crystal. The light energy of the flash is proportional to the energy of the X-ray photon. After the crystal the light is diffracted by the photo cathode which converts the light into a burst of electrons. The electron is accelerated by the series of dynodes (1-9). The positive potential raises with each dynode producing more and more electrons until the electron burst reaches the anode, where it causes a small current leading to a brief decline of voltage, a pulse. As

a downside for the scintillation detector, crystal fluorescence may be produced. The crystal fluorescence is caused by the fluorescence of the Iodine in the NaI-crystal. [17] [14]

3.5.10 Pulse Height Analyser

The pulse distribution data from detectors can be evaluated and modified in the pulse height analyser (PHA). The PHA distribution represents in percentage the energy distribution which enters the detector. For each analytical element a PHA window, the lower and the upper levels, for the pulse heights (intensities) are set. In the PHA window the analytical peak should have a Gaussian distribution and non-analytical signals should be removed to improve the analytical result. Non-analytical signals are such as electronic noise, pile up effect, crystal fluorescence, escape peaks and higher order peaks. Higher order peaks were discussed earlier in the chapter 3.5.8. "Analysing Crystal". [17] [14] [1] [10]

In PHA the pulse intensity is shown on Y-axis but the pulse distribution on X-axis varies between manufactures. In Rigaku system the energy distribution is from 50 to 500% where the energy of the measured element is assumed to be around 200%. In simple cases the PHA window is usually set to 100-300%. The lower limit removes electronic noise which is caused by the electronics behind the detector. The upper limit removes higher order energies and because higher order peaks show in the PHA around 400%. An example for this is shown below in Figure 16. In this work the 100-300% window was used for all elements. [10] [1] [18]
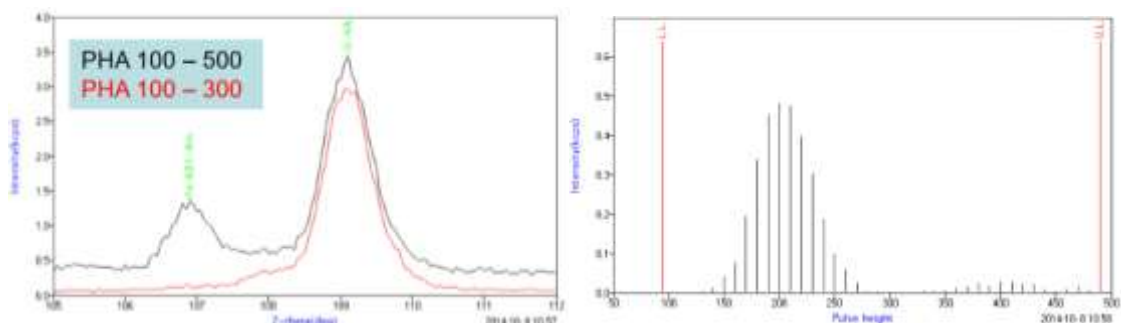
Figure 16. Si-KA result difference when PHA window is set to 100-300% and 100-500% (left picture) and how the PHA window looks like in Rigaku spectrometers (right picture). Higher order peak Fe-KB1-4th is eliminated and background lowers when the PHA window is set to 100-300%. [10]

Besides the electronic noise and higher order removals the pile up effect, crystal fluorescence and escape peaks can be seen in the pulse height analyser as well.

Pile Up Effect

The pile up effect may happen at very high count-rates (>2000 kcps) when instead of measuring all the incoming photons individually, the detector might measure two photons simultaneously, which leads to an additional peak after the main peak at around 400%. The pile up peak belongs to the signal but is most often removed since it can raise the instability of the analytical result. The pile up peak can be avoided by setting up the PHA window to 100-300% or by using a filter or attenuator (tube impact area limiter) or by decreasing the tube power. [10]

Crystal Fluorescence

The crystal fluorescence may happen when a sample excites photons with higher energy than the excitation energy of the electrons of a crystal. The crystal can either be from the analysing crystal or with heavier elements also from the NaI(Tl) crystal from the scintillation detector. The crystal fluorescence can be seen in PHA before the actual peak around 50-150% and should not be included to the signal. [10] [18] [17]

Escape Peak

In gas proportional counter detectors which use argon as counting gas, Ar-KA of argon may fluorescent, if X-rays with higher energy than the excitation energy of Ar-KA enter the detector. Those fluorescent X-rays can be seen as pulses in the PHA, proportional to the X-ray photon energy minus the excitation energy of Ar-KA (2.96 keV), and are referred to as escape peaks. As escape peak is a result from the analysed element and proportional, it can be included in the PHA window. Escape peak is seen in the PHA on the lower energy side of the actual peak. At low intensities the addition of an escape peak to a measurement can be beneficial if the peak is sufficient but as a down side the background might increase. [17] [10] [1]

4 Reagents, Instrumentation and Equipment

4.1 Reagents

Element reference solutions used in this work:

- 1000 mg/l K, Ca, Cr, Mn, Co, Cu, Zn, Cd, Tl and Pb standards in 0.5M HNO_3 matrixes
- 1000 mg/l Sn and Sb standards in 5M HCl matrixes
  Manufacturer: Romil. Trademark: PrimAg. Cautions: Health hazard and harmful.

4.2 Instrumentation

XRF spectrometer used in this work:

- Rigaku ZSX Primus II WDXRF spectrometer

4.3 Equipment

- Herzog Ht 40 pressing machine
- Retsch vibratory disc mill RS 200
- Heidolph MR 2002 magnetic stirrer
- Biohit 100-1000 µl automatic pipet
- mLINE 500-5000 µl automatic pipet

5 WDXRF Method Development

5.1 Steps of the Method Development

Method development was divided into three steps (Figure 17): preparation of the reliable calibration samples, founding the best measuring conditions with qualitative analysis and creation of the quantitative method.
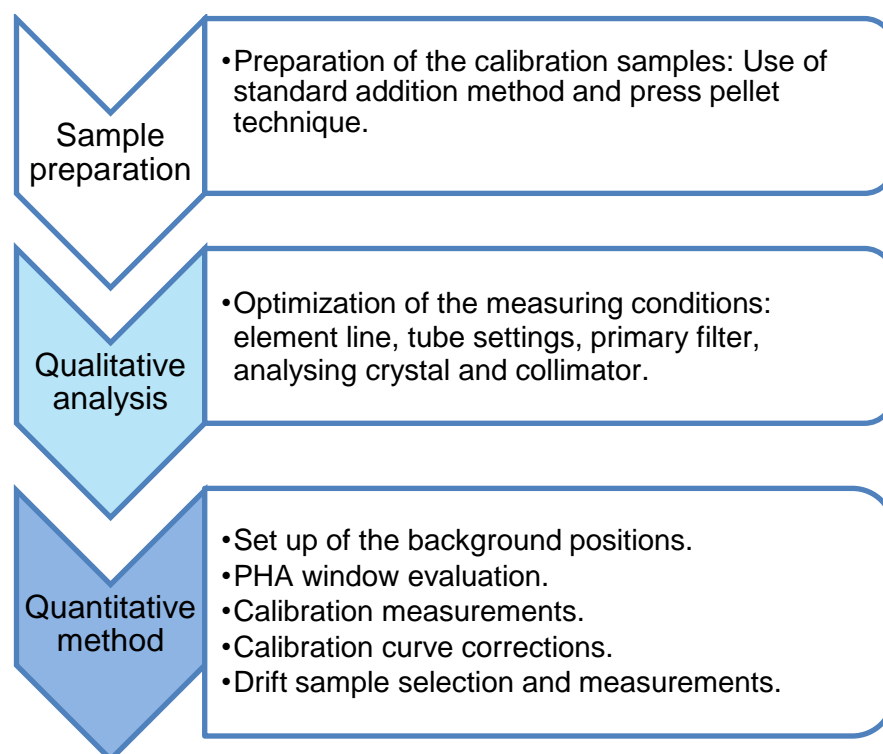

Sample preparation
• Preparation of the calibration samples: Use of standard addition method and press pellet technique.

Qualitative analysis
• Optimization of the measuring conditions: element line, tube settings, primary filter, analysing crystal and collimator.

Quantitative method
• Set up of the background positions.
• PHA window evaluation.
• Calibration measurements.
• Calibration curve corrections.
• Drift sample selection and measurements.

Figure 17. The three steps of the method development which are discussed in the next three sub-chapters.

The method included twelve elements to be calibrated: potassium (K), calcium (Ca), chromium (Cr), manganese (Mn), cobalt (Co), copper (Cu), zinc (Zn), cadmium (Cd), tin (Sn), antimony (Sb), thallium (Tl) and lead (Pb) with concentration range of 0-100 ppm. The elements were from quite wide atomic number (Z) spectrum: K have Z of 19 and Pb Z of 82. As in XRF the characteristic qualities of an element are determined by the atomic number, different matters were needed to take into consideration between the elements during the calibration.

5.2 Sample Preparation

5.2.1 Basic Principle of the Sample Preparation

The calibration samples were produced by using standard addition method: element standards were spiked (added) into a blank asphaltene sample in various concentrations leading to a calibration curve for each element. The idea was to dissolve the blank sample homogeneously into a sufficient amount of diluted element standards and air-dry in a fume hood and press the powder afterwards into a press pellet for the analysis. Advantages of the press pellet technique are that the technique do not destroy the sample or require to dilute the sample, which both are important qualities when analysing extremely low concentrations as in this work. Also the sample preparation is quick and easy. Another technique to prepare the samples would have been the fused bead technique but its high fusion temperatures could damage the sample leading to concentration losses and therefore the technique was not used.

5.2.2 Blank Sample

A blank sample was used as a matrix to the spiked standard concentrations. The blank sample had similar asphaltene-like chemical composition which is crucial in XRF. The blank sample was from the laboratory and was measured with ICP-OES to find out the starting concentrations for the spiked standards. The blank sample did not contain the calibrated elements or the concentrations were very low. The blank sample did contain rather high concentration of vanadium which disturbs the detection of chromium and will be discussed later in this thesis. However, more detailed information of the blank sample is classified and thus not included in this thesis.

5.2.3 Press Pellet Technique

The blank sample was coarse powder also containing larger chips and was grinded to fine powder with a grinding vessel as fine powder (small grain size) gives higher intensities and more stable results. For the grinding a zirconia grinding vessel was used. Potential contaminants from zirconia vessels are mostly zirconium but hafnium and magnesium for a lesser degree as well. Every vessel material has its own contaminant risks and therefore zirconia vessel was suitable for this work, as none of its possible contaminants were analytes in this work. [1]

The sample (powder) was pressed to pellets as pressed samples give higher intensities than loose powder samples. [10] The pellets were pressed with a Herzog Ht 40 pressing machine. The maximum pressing force of the machine is 400 kN. Prior to this work the asphaltene samples were pressed with force of 150 kN and with sample amount of 5 g. However, the samples tend to crack at times from the top surface and thus different pressing forces (50-150 kN) and sample amounts (3-5 g) were tested. 3 g sample with pressing force of 100 kN seemed to result for the most reproducible pellets. However, XRF analysis requires sufficient analysing depth for the X-rays to penetrate the sample properly. Therefore, 3, 4 and 5 g samples were pressed with 100 kN and measured with semi-quantitative WDXRF (Figure 18). Significant result differences were not found and 3 g of sample pressed with 100 kN force was chosen as the way to produce the samples.

Figure 18. 3, 4 and 5g of blank sample on top of 10ml of Boreox in aluminium cup pressed with 100kN.

For the base of the press pellets 10 ml (~3.4 g) of Boreox was used as a backing material in a 40 mm aluminium cup. Boreox is organic material which is highly stable under X-rays and is used to prevent X-rays from reaching the aluminium cup.

5.2.4 Sample Preparation Development

Prior to this work the sample preparation was tested in the laboratory with spiking element standards into ionized water and dissolving a blank sample into it. The wet sample was left into a fume hood overnight to dry and afterwards the dry powder was pressed into a press pellet. The extra volume from the ionized water was used to improve the uniform diffusion of the spiked elements in the sample. However, the sample did not dissolve into water very well but was found to dissolve into ethanol.

From that starting point the sample preparation testing was started with spiking 1, 2, 5, 10 and 20 ppm concentrations of thallium into ethanol and mixing with the blank sample. The samples were analysed with a qualitative analysing method. The results are shown in Figure 19.
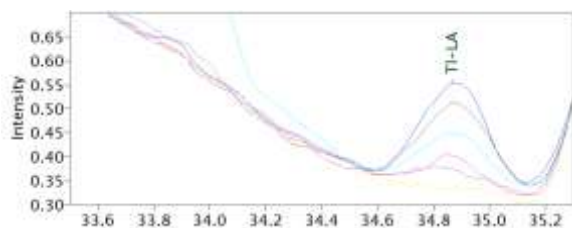
Figure 19. Results of spiked 1, 2, 5, 10 and 20ppm of Thallium compared against the blank (non-spiked) sample (yellow) by qualitative analysis.

The results showed successful separation between every sample even though the linearity did not match the concentrations perfectly. However, since the sample preparation method and the measuring parameters were not optimized yet, the results were taken as an indication that the sample preparation method could work.

5.2.5   Calibration Sample Preparation

In calibration sample preparation it is important to take into consideration that the analytes might interfere with each other. Overlapping elements and matrix effects might corrupt the calibration and possible interfering needs to be detected. Therefore, for a successful XRF calibration, it is essential to use alternating element concentrations in the calibration samples. That way the interferences will be observed as the relations between the concentrations of the analytes change between every sample. In this work there were 12 analytes, from a quite wide elemental spectrum, shown below in Table 3.

Table 3. Calibrated elements and their elemental and XRF qualities. [10]

Element	Atomic Number (Z)	Line	Crystal degree LiF(200)	Crystal degree LiF(220)
K	19	KA	136.69	-
Ca	20	KA	113.09	-
Cr	24	KA	69.36	107.11
Mn	25	KA	62.97	95.20
Co	27	KA	52.80	77.90
Cu	29	KA	45.03	65.56
Zn	30	KA	41.80	60.58
Cd	48	KA	15.31	21.72
Sn	50	KA	14.04	19.90
Sb	51	KA	13.46	19.07
Tl	81	LA	34.88	51.17
Pb	82	LA	33.92	48.73

In Table 3 it can be noticed that the crystal degree differences (resolution) between elements narrow significantly as the atomic number increases. The closeness of Cd, Sn and Sb and Tl and Pb was taken into consideration when the alternating concentrations were chosen.

The concentration range of the method was from 0 ppm to 100 ppm and eight calibration samples were made with spiked concentrations of 2, 5, 10, 20, 30, 40, 50 and 100 ppm alongside with non-spiked blank. The alternating element concentrations of the calibration samples are shown in Table 4.

Table 4. Element concentrations (ppm) of the calibration samples (Blank + 8 spiked calibration samples).

Calibration sample→

Element↓	Blank	1	2	3	4	5	6	7	8
K	0	**2**	5	10	20	30	40	50	100
Ca	0	**5**	10	20	30	40	50	100	2
Cr	0	**10**	20	30	40	50	100	2	5
Mn	0	**20**	30	40	50	100	2	5	10
Co	0	**30**	40	50	100	2	5	10	20
Cu	0	**40**	50	100	2	5	10	20	30
Zn	0	**50**	100	2	5	10	20	30	40
Cd	0	**100**	2	5	10	20	30	40	50
Sn	0	**5**	10	20	30	40	50	100	2
Sb	0	**20**	30	40	50	100	2	5	10
Tl	0	**40**	50	100	2	5	10	20	30
Pb	0	**100**	2	5	10	20	30	40	50

To achieve the concentrations shown above in Table 4, element standards were added to the blank sample. The used element standards were 1000 ppm as undiluted but for the lowest concentrations (2-20 ppm) the pipetting volumes would have been rather low for accurate pipetting and thus the standards were diluted to 1:10 with ionized water. However, the standards were used as undiluted with higher concentrations (30-100ppm) because the amount of pipetted water was wanted to keep minimal. Those choices resulted into the pipetting table shown in Table 5. The volumes were pipetted with two automatic pipettes. The volumes were calculated to be suitable for sample amount of 13 g.

Table 5. Pipetting volumes (ml) of the element standards into the calibration samples. Both 100 mg/l and 1000 mg/l standards were used to gain around 11 ml of the total standard volume for each sample.

Spiked volumes (ml)

13 g sample

Standard concentration→ 100 mg/l / 1000 mg/l

Sample→ Element↓	Blank	1	2	3	4	5	6	7	8
K	0	0,26	0,65	1,30	2,60	0,39	0,52	0,65	1,30
Ca	0	0,65	1,30	2,60	0,39	0,52	0,65	1,30	0,26
Cr	0	1,30	2,60	0,39	0,52	0,65	1,30	0,26	0,65
Mn	0	2,60	0,39	0,52	0,65	1,30	0,26	0,65	1,30
Co	0	0,39	0,52	0,65	1,30	0,26	0,65	1,30	2,60
Cu	0	0,52	0,65	1,30	0,26	0,65	1,30	2,60	0,39
Zn	0	0,65	1,30	0,26	0,65	1,30	2,60	0,39	0,52
Cd	0	1,30	0,26	0,65	1,30	2,60	0,39	0,52	0,65
Sn	0	0,65	1,30	2,60	0,39	0,52	0,65	1,30	0,26
Sb	0	2,60	0,39	0,52	0,65	1,30	0,26	0,65	1,30
Tl	0	0,52	0,65	1,30	0,26	0,65	1,30	2,60	0,39
Pb	0	1,30	0,26	0,65	1,30	2,60	0,39	0,52	0,65
Total (ml)	0	12,74	10,27	12,74	10,27	12,74	10,27	12,74	10,27

Each element standard was separately pipetted into 30 ml of ethanol in a 400 ml plastic bottle and 13 g of the blank sample was mixed in with help of a plastic funnel. On the bottom of the bottle a magnetic stirrer was used. The magnetic stirrer and the funnel were flushed with 5 ml ethanol afterwards. The samples were left to a fume hood to air-dry. After two days the samples were moved to a mortar (Figure 20) and the bottom of the bottle was flushed with 5 ml of ethanol and the sample was left to dry in the mortar for overnight until finished.

Figure 20. The dried samples were easy to drop from the bottom of the used plastic bottle to a mortar. The sample broke from bigger pieces (left picture) to fine dusty dry powder (right picture) with just lightly pressing with a plastic spoon.

5.3   Qualitative Analysis

Qualitative analysis was used to optimize the measuring parameters and observe possible peak overlays. The qualitative analysis scans element line intensities from a set range of crystal degrees by a set degrees/min speed and the found peaks (wavelength) can be identified with the instrument software. Individual qualitative methods can be created to each analyte and different tube voltage/current, filter, crystal and collimator settings can be tested. In qualitative method result spectra can be visually evaluated and the spectra can be overlaid and compared to ease the evaluation.

The qualitative tests for the analytes were started with 50 kV/60 mA Rh tube power, S2 (narrow) collimator, Lif(200) crystal and PHA window of 100-300%. Strongest element lines (KA except LA for Pb and Tl) were preferred as the concentrations were rather low. The detector was determined automatically by the wavelength of the element (proportional counter for K and Ca and scintillation counter for the rest).

At first different tube power settings were tested. Higher power settings seemed to gain higher peak-to-background ratios and by visual estimation different tube power settings were chosen. An example with K-KA is shown below in Figure 21.
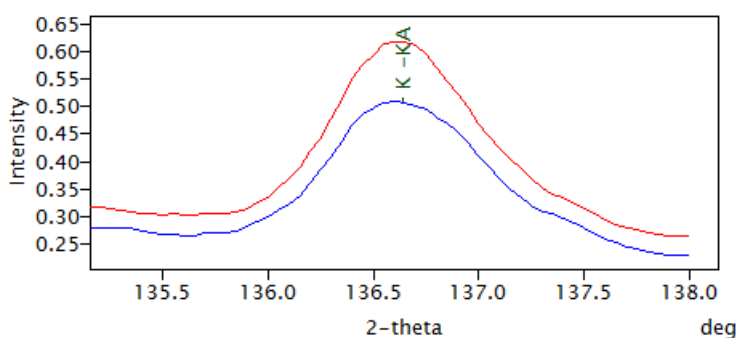
Figure 21. K-KA spiked 10 ppm with LiF(200) and S2 collimator. Comparison between 50kV/60mA (blue) and 60 kV/66 mA (red) tube settings.

Collimator S2 was chosen for all elements since it gained the best resolution but also enough intensity. If the intensities in the low concentrations would have been too low, wider S4 collimator could have been an option for the lighter elements (K, Ca, Mn etc.).

For the selection of the crystal Lif(200) and Lif(220) were available where Lif(220) produces higher resolution. [17] In this work Lif(220) was possible to choose for all the other elements except for K and Ca. Lif(220) were chosen for Cr-KA, Sb-KA and Pb-LA for

extra resolution. Cr-KA is positioned close to V-KB1 and the blank sample contained rather high vanadium concentration and thus the most resolution was needed. For Pb-LA the peak-to-background ratio was better with LiF(220) which is shown below in Figure 22.
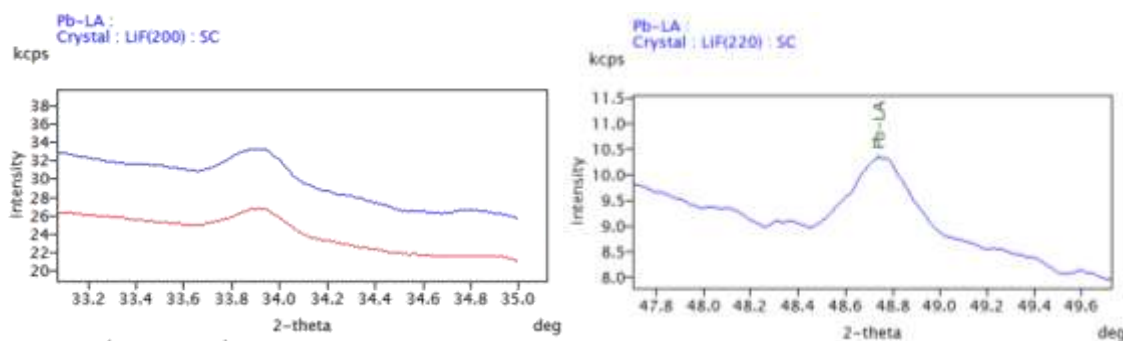

Figure 22. Pb-LA parameter testing with spiked 20 ppm calibration sample. The spectrum on left is measured with LiF(200) and with tube power of both 50 kV/60 mA (red line) and 60 kV/60 mA (blue line). The spectre on right is measured with LiF(220) and with tube power of 60 kV/60 mA.

A few filters were applied: Ni400 for Cd-KA, Sn-KA and Sb-KA to block the Rh-KA Compton from Bremsspectrum (Chapter 3.5.5 "Bremsspectrum"), Ni40 to Tl-LA to improve the peak-to-background ratio and Al125 to Cr-Ka to improve the peak-to-background ratio as well. All the chosen parameters are shown below in Table 6.

Table 6. Chosen parameters.

El. Line	Target	kV-mA	Filter	Slit	Crystal	Detector	PHA (%)
K-KA	Rh	50-80	-	S2	Lif(200)	PC	100-300
Ca-KA	Rh	50-80	-	S2	Lif(200)	PC	100-300
Cr-KA	Rh	50-60	Al125	S2	Lif(220)	SC	100-300
Mn-KA	Rh	60-60	-	S2	Lif(200)	SC	100-300
Co-KA	Rh	60-66	-	S2	Lif(200)	SC	100-300
Cu-KA	Rh	60-60	-	S2	Lif(200)	SC	100-300
Zn-KA	Rh	60-66	-	S2	Lif(200)	SC	100-300
Cd-KA	Rh	60-66	Ni400	S2	Lif(200)	SC	100-300
Sn-KA	Rh	60-60	Ni400	S2	Lif(200)	SC	100-300
Sb-KA	Rh	60-50	Ni400	S2	Lif(220)	SC	100-300
Tl-LA	Rh	60-66	Ni40	S2	Lif(200)	SC	100-300
Pb-LA	Rh	60-60	-	S2	Lif(220)	SC	100-300

5.3.1 Overlaps

The qualitative analysis was also used to check for any overlaps. The found overlaps, partial overlaps and nearby peaks had minor intensities in the blank sample and were not assumed to affect the calibration except for V-KB1 overlay on measured Cr-KA which is discussed more in chapter 5.4.6 "Challenges in the calibration of chromium". The theoretical and found overlaps, partial overlaps and nearby by peaks are listed below in Table 7.

Table 7. Theoretical (literature) and found overlaps, partial overlaps and nearby by peaks for the measured elements in the calibration samples. [1]

Element Line	Theoretical overlaps	Found Overlaps/nearby peaks from the sample
K-KA	-	Cd-LB1
Ca-KA	K-KB, Sn-LB	-
Cr-KA	V-KB, Ba-LY, Zr-KA, Pr-LB, La-LB, Ce-LB	V-KB1, Pm-LA
Mn-KA	Cr-KB, Ba-LY	Cr-KB1, Eu-LA
Co-KA	Fe-KB, Er-LA, Hf-L, Tb-LB1, Nd-LY	Er-LA, Tb-LB1
Cu-KA	Ta-LA, Ni-KB, W-LA, Hf-Ln	Tm-LB1, Ta-LA
Zn-KA	Cu-KA, Cu-KB, W-LA, Ta-Ln	Re-LA, Lu-LB1
Cd-KA	-	Pd-KB1, Rh-KB1
Sn-KA	Ag-KB1	Ag-KB1
Sb-KA	Cd-KB1	Cd-KB1
Tl-LA	-	Ga-KB1, Os-LB1
Pb-LA	As-KA	As-KA

The effect of a possible overlap is based on its concentration in the sample. If an element line next to a measured element have minor intensity, it most likely will not affect the calibration, for example Cr-KB1 next to the calibrated Mn-KA line shown below in Figure 23. However, higher resolution analysing crystal Lif(220) could have been used in this case if higher resolution between Cr-KB1 and Mn-KA would have been needed.
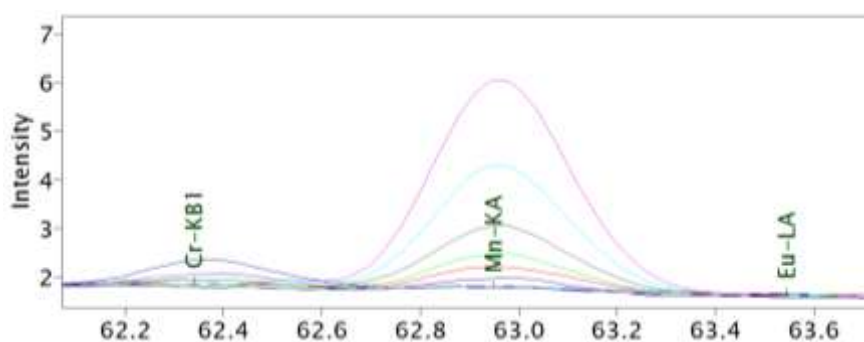
Figure 23. Qualitative analysis result of Mn-KA (0-100 ppm). Intensity (kcps) on y-axis and 2-theta (crystal degrees) on x-axis. Chromium (0-100 ppm) had its KB1 line next the Mn-Ka line.

5.4   Quantitative Method

In the quantitative method sample intensities are converted into concentrations by calibration curve data formed by measured reference standards and possible calibration curve corrections. In the quantitative method also measuring conditions can be fine-tuned if needed and background positions and PHA windows are set. In the quantitative method only the set background position(s) and the peak position are measured. After the calibration measurements drift samples were selected and measured to ensure the method longevity. In this calibration eight calibration samples and a blank sample were used and for each sample a duplicate sample was used.

5.4.1   Empirical Method

For the quantitative method an empirical calibration method was used. The empirical calibration method is a comparative method which forms calibration curves by the relationship between input calibration sample concentrations and their measured intensities. Since unknown samples are measured against the stored calibration curves, calibration samples need to be representative of unknown samples. Successful calibration of the empirical method produces precise results but cannot be used in situations where the sample composition varies between samples. The empirical method does not require all the elements in the sample to be analysed. [11] [14]

Fundamental Parameters Method

Another quantitative method is the fundamental parameters (FP) method which uses mathematical models and the sample intensities in the measurements. The FP calibration needs less calibration samples, even just one standard can be sufficient enough. Also the calibration samples do not need be representative to the unknown samples and thus, the FP method can be rather versatile. However, due to the mathematical approach the FP method is more restrictive. 100% of the sample composition is needed to be known. Therefore, all the unmeasured elements need to be either inputted or balanced (fill the sample composition to 100%). Also, in powder samples any grain size differences will cause error. The restrictive qualities of the FP method were the reason why the empirical method was preferred to use in this work. [11] [13] [18]

5.4.2   Measuring Condition Optimization

In the measuring condition optimization the highest and the lowest calibration concentrations for the analytes were measured from the calibration samples. The samples were run with the parameters found best at the qualitative analysis. Both qualitative and PHA scan were measured. From the qualitative scan the background positions were set and from the PHA scan PHA window was analysed and set.

Background Positions

In qualitative analysis only the peak and the set background positions are measured and the net intensity is calculated. Background positions are always needed unless the background is insignificant compared to the peak intensity in high concentration analyses.

There are a few different methods for the setup of the background positions: One-point, Two-point and multi-point methods such as quadratic and Lorentz function. In One-point method one background point is set and the method is used when the background near the peak is flat and steady. One-point method was used with half of the elements in this work, for example with Zn-KA shown below in Figure 24.
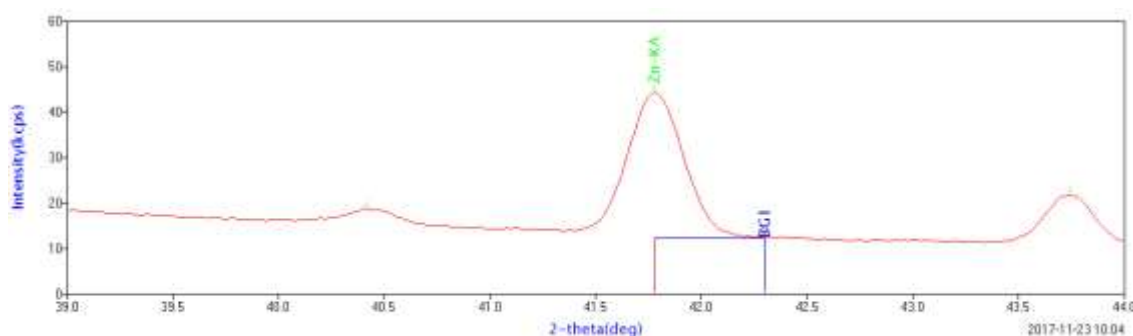
Figure 24. One-point background setup with 100 ppm Zn-KA.

In two-point method a background point from both sides of the peak are measured creating a straight line and the background intensity is calculated from the point of the peak from the line. Two-point method is good to use when the background near the peak is inclined. The two-point method was used with five of the elements in this work, for example with Sn-KA shown in Figure 25.
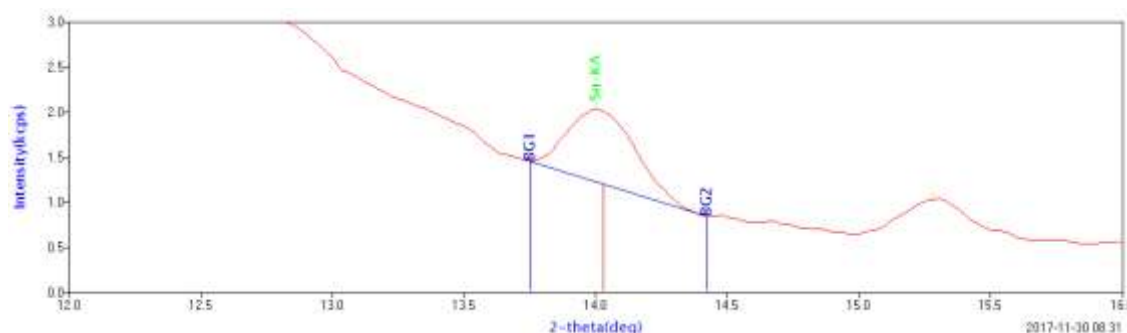
Figure 25. Two-point background setup with 100 ppm Sn-KA.

In quadratic method three or more background points are measured and a quadratic function is created. The quadratic method can be used like the two-point method in inclined positions or to improve measurements with overlapping peaks. In this work the quadratic method was used for Sn-KA as a test to improve the calibration results but no significant changes were obtained. The quadratic method could also been used in this work with Cr-KA which is discussed more in the chapter 5.4.6 "Challenges in the calibration of chromium". Below in Table 8 the used background methods in this work are shown.

Table 8. Background position set-ups for the calibration.

Element line	Background point method
K-KA	Two-point
Ca-KA	Two-point
Cr-KA	One-point
Mn-KA	One-point
Cu-KA	One-point
Co-KA	One-point
Zn-KA	One-point
Cd-KA	Two-point
Sn-KA	Two-point
Sb-KA	Three-point quadratic
Tl-LA	Two-point
Pb-LA	One-point

PHA Window

PHA window of 100-300% was considered sufficient for every element. The lower limit of 100% cuts of unnecessary electrical noises and the 300% upper limit cuts of crystal fluorescence and higher order peaks. Below the set PHA window for K-KA is shown in Figure 26.
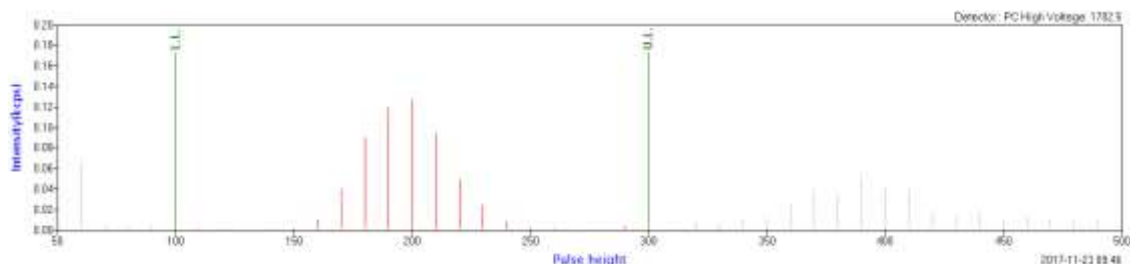
Figure 26. PHA window set to 100-300% for K-KA (2 ppm). Around 400% higher order peak is seen.

5.4.3   Calibration Measurements

The calibrated element lines were measured all with same measuring time settings shown below in Table 9.

Table 9. Calibration measuring times and repetition multiplier for all elements.

Peak measuring time	Background point measuring time	Repetition multiplier
40 s	20 s	2x

Repetition multiplier was used with multiplier of two meaning that the element peak and the background point(s) was/were analysed twice and the average intensities were used to compose the calibration curves. Calibration samples in the auto sampler of the spectrometer are shown in Figure 27.

Figure 27. The calibration samples ready to be measured in the auto sampler of the instrument (blank and 8 calibration samples with their duplicates).

5.4.4 Calibration Curves

Mostly the measured calibration curves had rather high accuracy and did not require any corrections. Also the measured duplicates did not show large difference between the samples. For some curves the duplicates did not show almost any difference at all. The most successful curve (Cu-KA) is shown in Figure 28.
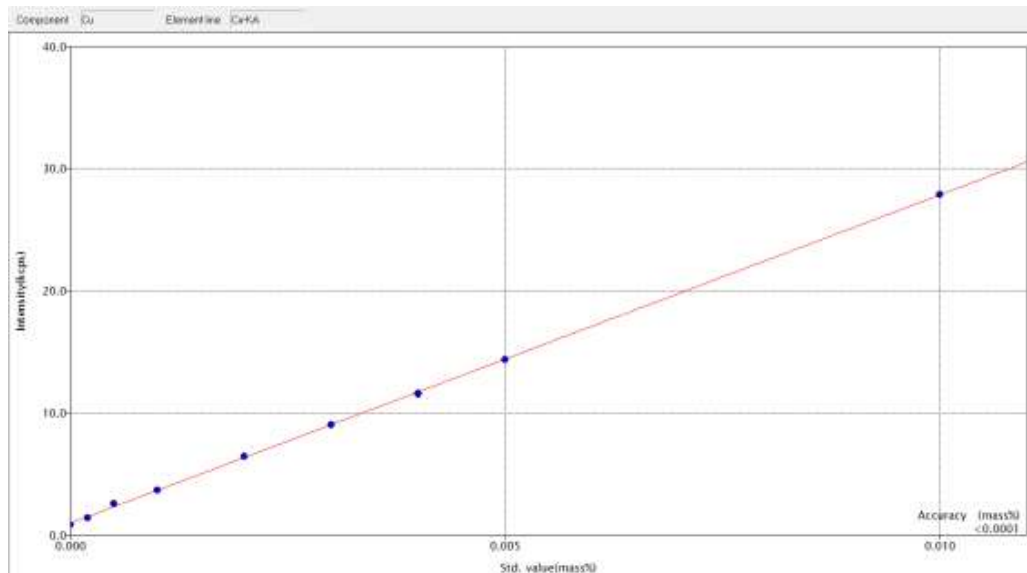
Figure 28. The calibration curve of Cu-KA (RSD <0.0001%).

For Tl, Pb, Cd, and Zn the curves had quite high accuracy as well (RSD 0.0001-0.0002%) and showed only minor deviation between concentrations and almost zero deviation between duplicates. The calibration curve of the Pb-LA is shown in Figure 29.
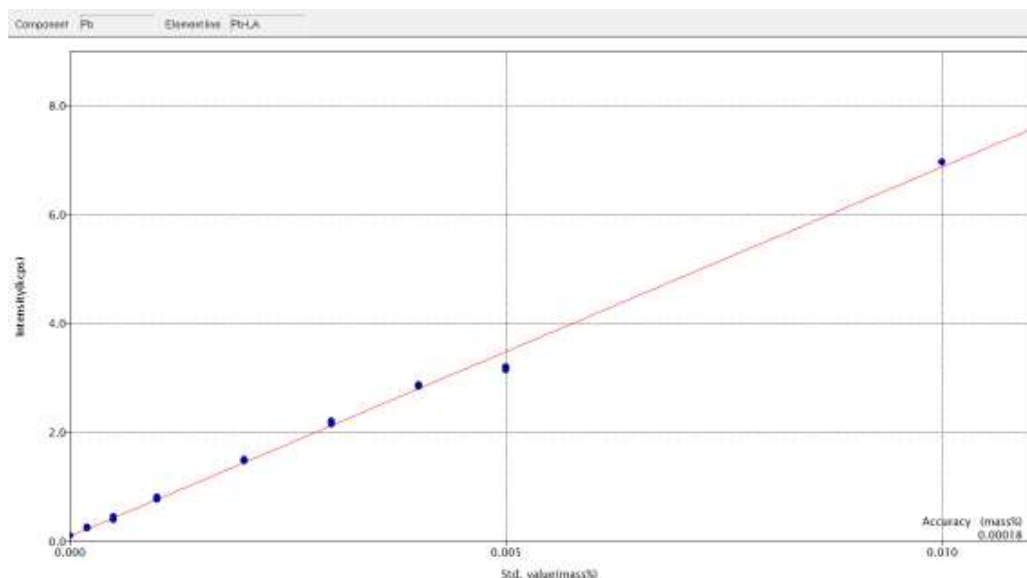
Figure 29. The calibration curve of Pb-LA.

For Ca-KA, the curve was rather accurate as well (RSD 0.0003%) but the second blank showed some deviation between the sample and the duplicate. The curve is shown below in Figure 30.
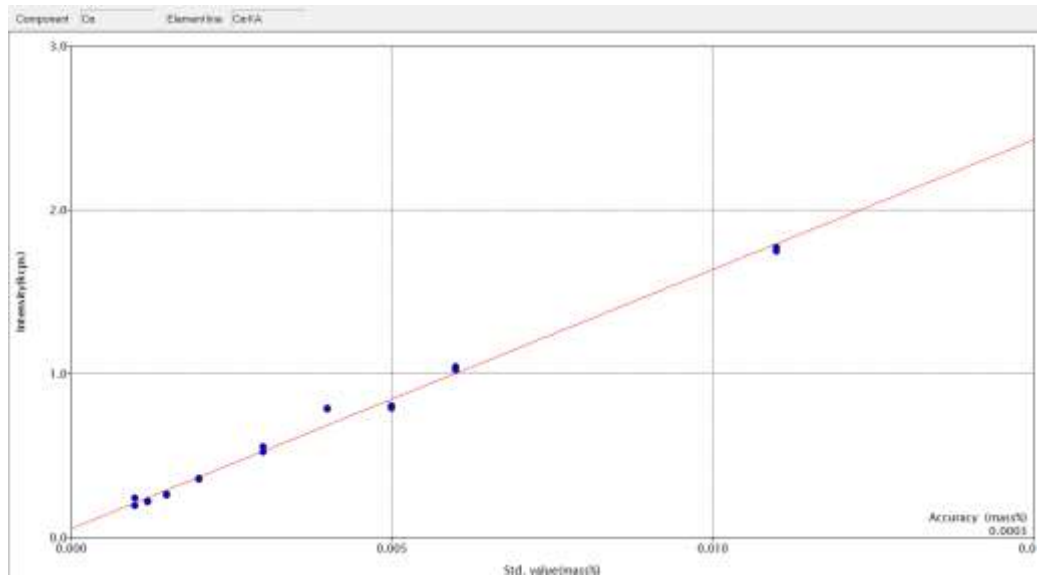
Figure 30. The calibration curve of Ca-KA.

For Mn-KA the curve was very good from 0-10 ppm and quite good for 0-40 ppm but there was quite lot of deviation between the 50 ppm and 100 ppm samples. Since the lowest concentrations were the most important for this calibration, no corrections were made. The curve is shown below in Figure 31.
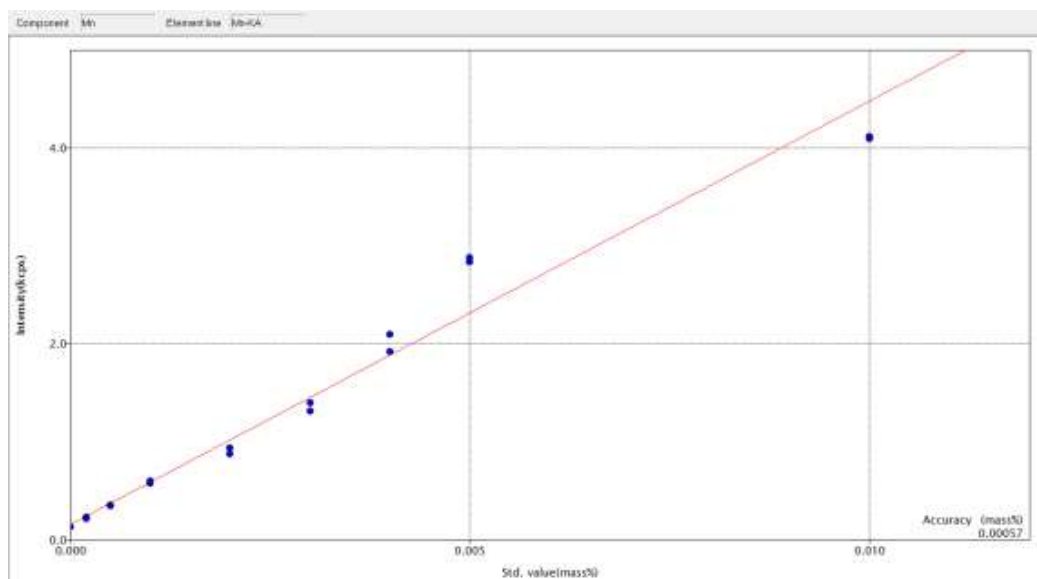
Figure 31. The calibration curve of Mn-KA (RSD 0.0006%)

From the calibration curves of Sb, Sn and K, one concentration point was deleted from each curve due to poor accuracy. The curve for Sn-KA is shown below in Figure 32.
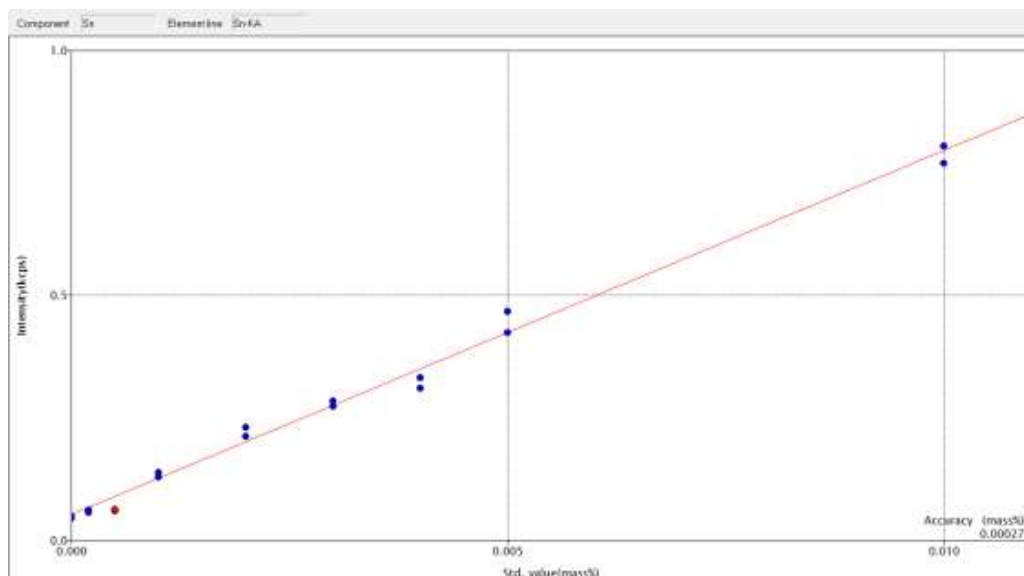
Figure 32. The calibration curve of Sn-KA (RSD 0.0003%). The third point (5 ppm) samples did not differentiate from the 2 ppm samples and were deleted.

For Cr-KA and Co-KA calibration corrections were made which is discussed in the next chapter 5.4.5. "Calibration curve corrections". All the calibration curves can be seen in the appendix 1 "Calibration curves".

5.4.5 Calibration Curve Corrections

After the calibration measurements the calibration curves may need to be corrected to correspond better the actual sample values with calibration corrections. Two types of corrections can be applied: Line overlap and matrix corrections. When using empirical method it is recommended to limit the number of applied corrections by the number of used calibration samples by the following formula (equation 3):

$$N = 2k + 1 \text{ , where} \tag{3}$$

N = number of standards
k = degrees of freedom.

Degrees of freedom include the stored information of the curve; offset, slope, overlap corrections and matrix corrections. In this work the total of nine standards (a blank sample and eight calibration samples) were used which would result that according to the formula no more than two corrections should be applied for each calibration curve beside the stored slope and intercept. [10]

Line Overlap Corrections

Line overlap corrections can correct element lines that either entirely or partly overlap with the element line of interest, thus incorrectly increasing the measured element intensity. Overlapping lines can be from another calibrated element or from element outside the calibration, a matrix element. Overlapping lines can be K, L, M etc. element lines but also an escape peak from a matrix element can overlap. In the empirical method overlap corrections are applied by concentration, therefore the concentrations of the overlapping elements have to be known (inputted) unlike in the fundamental parameters method where the overlap corrections are applied by the measured intensities. [11] [13]

In this work line overlap correction was applied to Cr-KA because it was overlapped with vanadium KB1 line (more in the chapter 5.4.6 "Challenges in the calibration of chromium"). The vanadium concentration was inputted to the method and the correction was applied for the measured calibration curve (Figure 33).
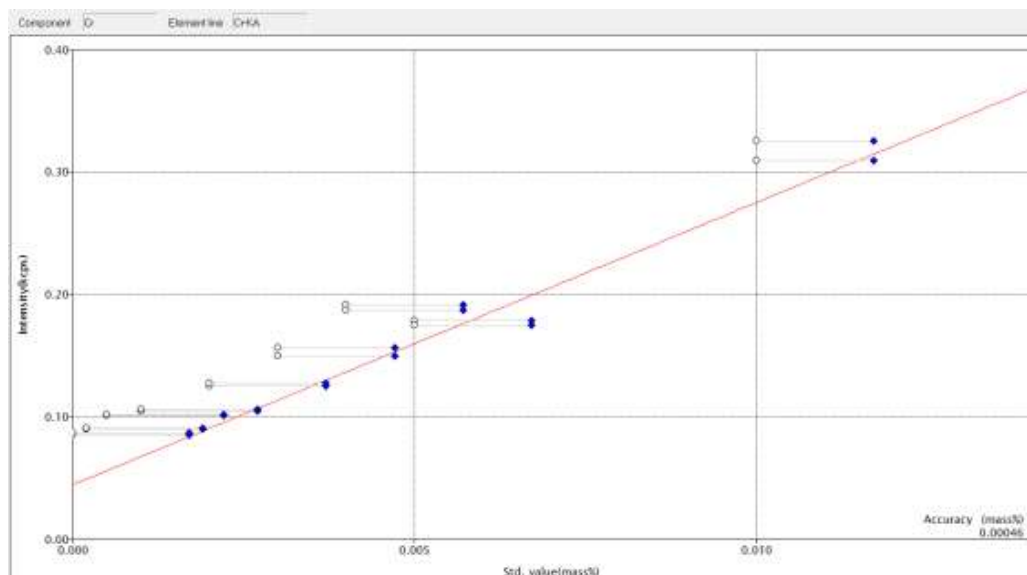
Figure 33. The calibration curve of Cr-KA with vanadium overlap correction.

In the future the vanadium concentration can be inputted separately before each sample analysis to match the correct vanadium concentration.

Matrix Correction

Matrix corrections correct effects of the sample matrix with regression calculations. In the sample matrix the element intensities are influenced by each during the measurements which more or less disturb the measurement results. The matrix effects include both absorption and enhancement effects. All elements absorb X-ray fluorescence produced by other elements, referred as the absorption effect. The absorption effect intensity depends on the element (atomic number and wavelength) and its concentration in the sample. Sometimes an element can fluorescent from the fluorescence radiation of the other sample elements causing extra fluorescence for the element which is referred as the enhancement effect. The enhancement can happen when the enhancing element line have slightly higher binding energy than the analyte. Therefore in absorption the emitting element "loses" fluorescence intensity whereas in enhancement "extra intensity" is gained. Below in Figure 34 the matrix effects are illustrated. [11] [10] [13]
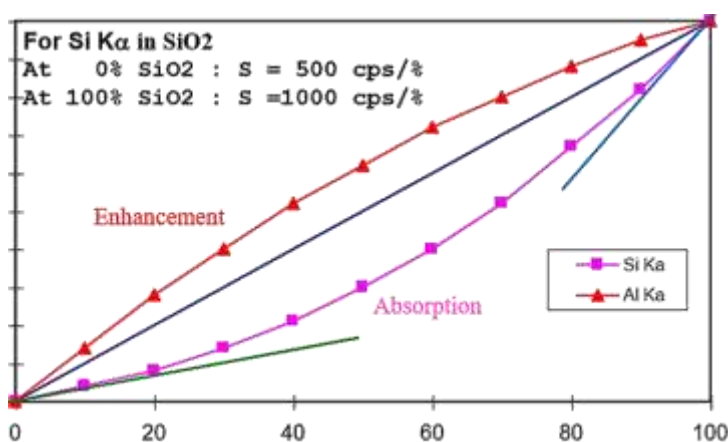
Figure 34. The distinctive figures of absorption and enhancement effects. [10]

In this work matrix correction was applied to Co-KA since there was rather high deviation between the middle concentrations (20-50 ppm) and was believed to be matrix error. In the empirical method absorb/enhancement correction can be applied by concentration from either a measured element or a matrix element. For Co-KA the concentrations of the other elements were checked from the calibration points which differentiated the most from the curve. By testing different corrections, the Co-KA was the most influenced by

the 50 and 100 ppm concentrations of Tl, Zn and Cd and the absorb/enhancement correction was applied, as shown below in Figure 35.
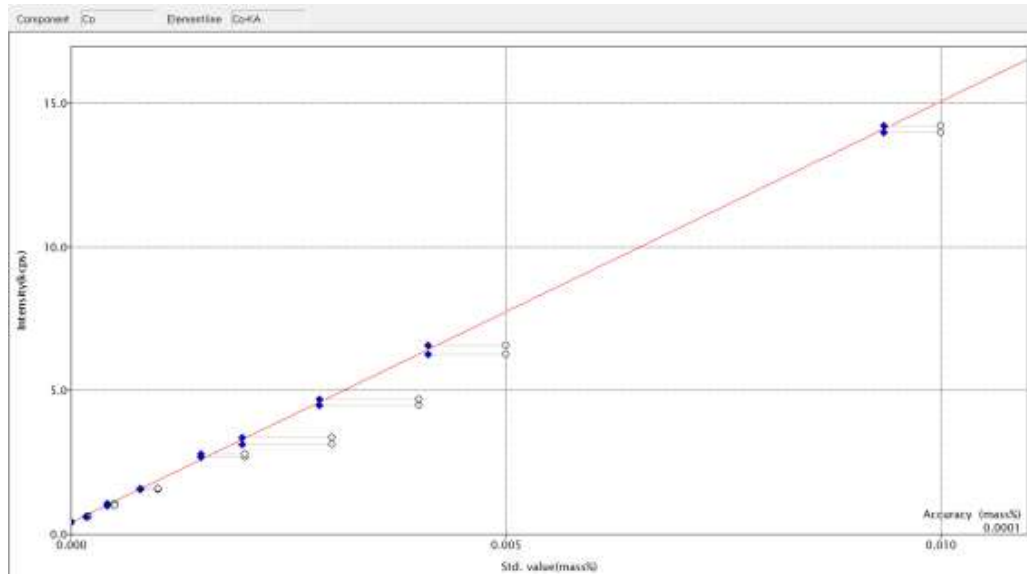

Figure 35. Co-KA calibration curve with Tl, Zn and Cd absorb/enhancement corrections.

5.4.6   Challenges in the Calibration of Chromium

Chromium was the most challenging element in this work to be calibrated as the Cr-KA line was overlapped by V-KB1 and the blank sample contained rather high concentration of vanadium. The V-KB1 line was chosen to be overlap corrected by concentration to produce proper results for Cr-KA. However, the overlap was rather major and it was concerned that the correction might not be enough for the method to be able to measure accurate results for Cr-KA. Below the overlap is shown in Figure 36.
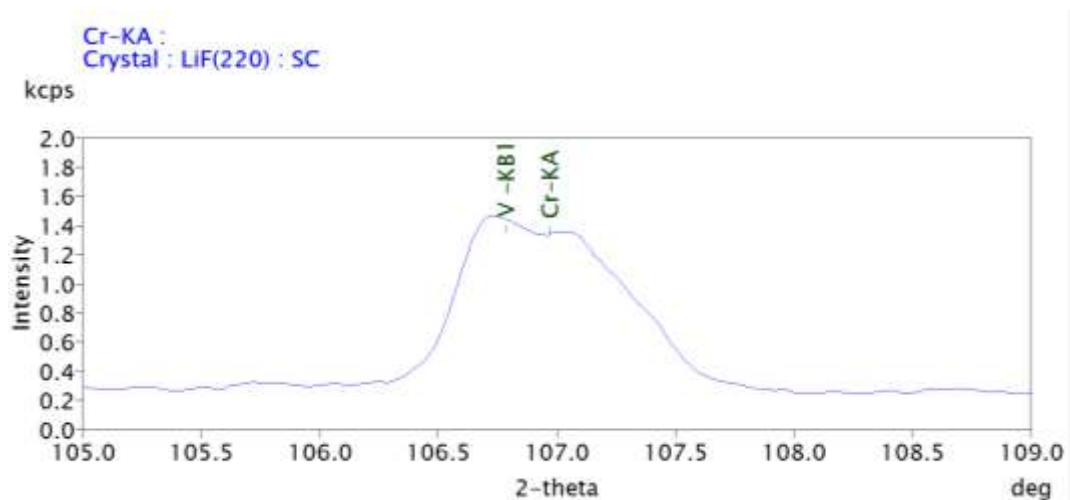
Figure 36. Cr-KA overlapping with V-KB1 with 100 ppm Cr calibration sample. With Lif220, 50 kV/60 mA and al125 a small separation was able to be seen.

However, there were quite many alternative measuring and correction options for the detection of the Cr-KA. One improvement would have been different background position set up. The used background point method was the one-point method where only one background point is used. However, to identify the vanadium overlapping a multi-point background point method could have been more accurate. A multi-point method Lorentz function could have been used which is a multi-point function especially for smaller peak on the side on a larger peak, as shown below in Figure 37. [18]
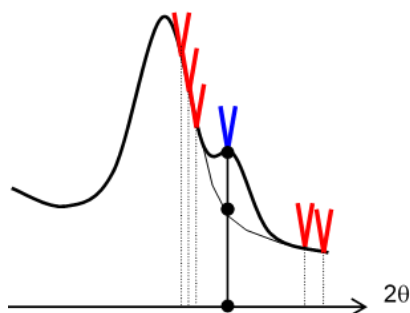
Figure 37. The Lorenz function. Red points are measured background points and the blue is the measured peak position. [18]

The most concerned matter in the vanadium overlap correction was the constantly changing concentrations of vanadium in the samples. The overlap correction might not be accurate when the concentration changes. If vanadium would have been added to the calibration as a calibrated element a proper overlap correction coefficient could have been determined. Also the same could have been done with just spiking only vanadium and chromium into separated test samples.

The chromium could also have been analysed with a different element line. The measuring of Cr-KB1 was tried in the qualitative analysis but the intensities were rather low and therefore the line was not used. However, there were not any overlaps for the Cr-KB1 and the method could have worked accurately with higher concentrations (+20 ppm).

One option for the detection of the Cr-KA would have been detection with a higher resolution crystal (LiF420). With higher resolution crystal the peaks of vanadium and chromium could have been separated properly. Disadvantage of the crystal would have been lower intensities. However, the instrument used in this work did not contain that particular crystal and therefore it was not able to be tested.

5.4.7   Drift Correction

The calibration accuracy is maintained with drift correction. The drift correction samples are chosen and measured after the calibration samples. The drift correction is needed because the x-ray tube and the detectors tend to lose intensity and sensitivity overtime. The intensities might also be affected by any performed service work. The intensity changes are not equal to all elements and each element need to have an own individual drift correction intensity to be corrected against with. Generally light elements are more influenced by the drift than heavier elements. [19]

For drift samples there are no other limitations than that they must be stable over long periods of time and their intensities have to correspond the calibration intensities. For the drift sample material glass samples are widely recommended due to their stability and were used in this work as well. Another rather stable option could have been metal samples. Also the calibration samples can be used as drift samples if they are stable. However, in this work the calibration samples were press pellets which are not stable enough. [18]

Drift correction can be set with just one or two drift samples for one calibrated element. If one drift sample is used, its intensity is preferred to be about halfway from the calibration curve. When two drift samples are used they are preferred to be a low and a high point intensity from the calibration curve. [18] In this work one drift sample intensity was used for each calibrated element since the calibration intensity range was rather narrow.

Five glass drift samples from Fluxana were tested: Flx-O9, Flx-O10, Flx-S13, Flx-Z1 and Flx-Z2. The samples were already in use or to be used in the laboratory and were not exclusively ordered. The sample intensities were measured in the quantitative method to find comparable sample intensities with the same measuring parameters that were used for the calibration samples. There are three different options to do the drift correction: The measuring condition can be either direct, indirect or other common measuring condition, explained in Table 10.

Table 10. The drift correction can be done with three different measuring conditions.

Direct measuring condition	The drift sample uses the same measuring condition as the measured element line in the method uses, for example: K-KA drift for K-KA.
Indirect measuring condition	The drift sample uses the same measuring condition as another measured element line in the method uses, for example: Ca-KA drift for K-KA.
Other common measuring condition	The drift sample uses a measuring condition of a nearby peak outside of the measured element lines, for example: Cr-KB1 for Mn-KA.

Direct measuring condition is the easiest option: if the drift sample intensity is in the acceptable range right away, it can be used directly. Indirect measuring condition is rather easy as well, another measuring condition from the method can be used as a replace. However, indirect measuring condition requires that the same measuring parameters have been used between the elements. It also requires that they both belong to the same elemental group. Indirect drift correction was used for example with Ca-KA shown below in Figure 38. The same line was used to K-KA drift as direct drift as well.
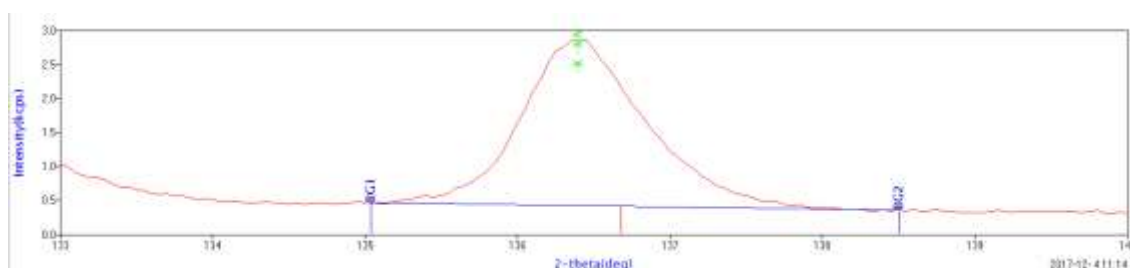
Figure 38. K-KA drift line was used directly for K-KA and indirectly for Ca-KA drift correction.

The drift correction in this work could have been accomplished with just direct and indirect measuring conditions but sufficient intensity of thallium was not found in the drift samples. Therefore, also other measuring condition drift method was used. Other common measuring conditions are created in a parallel method where the measuring condition is classified as a common line which will then be found and chosen in the actual method. The peak position is changed to measure a nearby peak with an appropriate

intensity and also the background point/points are changed if needed. Alongside with thallium, other common measuring condition drifts were used with Mn-KA and Pb-LA to achieve more suitable intensities. The peak position change of Mn-KA is shown below in Figure 39.
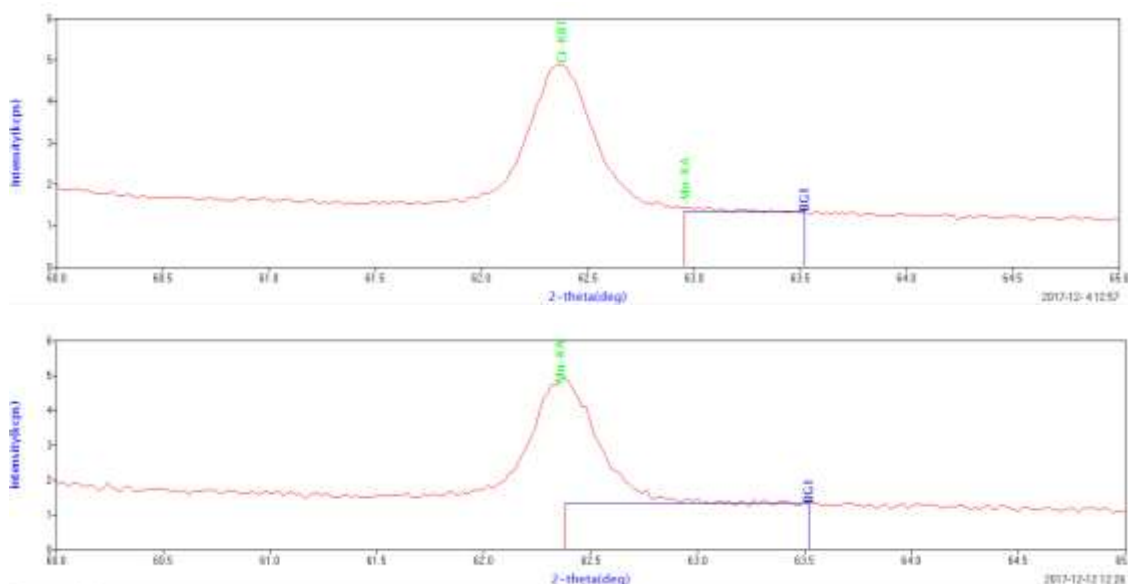

Figure 39. Mn-KA was moved to measure Cr-KB1 as the drift intensity.

In this work the intensities were rather low and the used drift samples were mostly aimed to higher intensities. Therefore, a few compromises had to be made in selection. Below in Table 11 the selected drift choices are shown.

Table 11. The drift samples were aimed to represent the calibrated element´s intensity range: The highest (100 ppm) calibration intensity is seen on the second column and the drift sample intensity on the third.

Element line	100 ppm net intensity (kcps)	Drift sample net intensity (kcps)	Drift sample	Drift element line	Drift type
K-KA	1	3	Flx-O9	K-KA	direct
Ca-KA	2	3	Flx-O9	K-KA	indirect
Cr-KA	0.3	1	Flx-O10	Cr-KA	direct
Mn-KA	4	6	Flx-O10	Cr-KB1	nearby peak
Cu-KA	28	34	Flx-S13	Mn-KA	indirect
Co-KA	14	70	Flx-Z2	Zn-KA	indirect
Zn-KA	32	70	Flx-Z2	Zn-KA	direct
Cd-KA	1	15	Flx-S13	Cd-KA	direct
Sn-KA	1	15	Flx-S13	Sn-KA	direct
Sb-KA	0.4	4	Flx-S13	Sb-KA	direct
Tl-LA	4	1	Flx-Z2	Pb-LA	nearby peak
Pb-LA	7	18	Flx-O10	Pb-LA2	nearby peak

6   Conclusion

The objective of this work was to calibrate a specialised quantitative method for asphal-tene samples for twelve elements (K, Ca, Cr, Mn, Co, Cu, Zn, Cd, Sn, Sb, Tl and Pb) with a calibration range of 0 to 100 ppm. The lower limit was determined by the concen-trations of the used blank sample. The method development included preparation of re-liable calibration samples and creation of an accurate quantitative method tailored for asphaltene samples. A reproducible sample preparation method was created and linear calibration samples were produced with standard addition method. Optimized measuring conditions were found which were also backed by expert literature. Rather high accuracy calibration curves were obtained (RSD <0.0001-0.0006%). The longevity of the method was ensured with proper selection and measurements of drift samples. However, time for testing the method was restricted and in the future the method will be further tested and validated.

In the calibration curves a few points were deleted which often is not the preferred way. Calibration curve corrections were applied to Co-KA and Cr-KA but the recommended number of applied corrections was exceeded with Co-KA. Also the applied vanadium overlap correction for Cr-KA might not be sufficient enough for accurate results. There are a lot of options during the method development and the most suitable options were tried to be found and applied. However, when creating a specialised quantitative XRF method, both profound understanding of the analysis and experience are needed for accurate and reliable calibration, especially in the lower concentration range with multiple analytes. Also extensive sample preparation and measuring condition testing can be very time consuming. However, after the calibration only check samples and drift correction are needed to maintain the method.

For improved results more thorough measuring condition experimentation and evalua-tion could have been done. Also testing the method more could have been beneficial. To ease the drift sample selection same measuring parameters between calibrated ele-ments could have been used more which would have allowed to use more the indirect drift correction.

7 References

[1] J. Willis, C. Feather and K. Turner, Guidelines for XRF analysis, Cape Town: James Willis Consultants, 2014.

[2] Neste, "Porvoo Refinery," [Online]. Available: https://www.neste.com/en/porvoo-refinery. [Accessed 19 January 2018].

[3] O. Wiki, "OilField Wiki," 2016. [Online]. Available: http://oilfieldwiki.com/wiki/Asphaltenes. [Accessed 17 January 2018].

[4] *Visit to the SDA-unit in Porvoo refinery,* 2017.

[5] Neste, "Powerplant arangement between Neste, Veolia and Borealis closed," *Stock exchange release,* p. 1, 16 March 2016.

[6] Neste, "Neste Who We Are," Neste, 2017. [Online]. Available: https://www.neste.com/en/corporate-info/who-we-are-0. [Accessed 28 December 2017].

[7] CBI, "What we do / Solvent deasphalting (SDA)," January 2018. [Online]. Available: https://www.cbi.com/What-We-Do/Technology/Refining/Residue-Upgrading/Deasphalting. [Accessed 19 January 2018].

[8] I. Alberta, Artist, *Innovative Asphaltene in Bitumen Measurement.* [Art].

[9] S. International, "PetroWiki," 15 January 2018. [Online]. Available: http://petrowiki.org/Asphaltenes_and_waxes. [Accessed 19 January 2018].

[10] P. D. Pape, Writer, *Basic Principles of WDXRF.* [Performance]. Rigaku, 2014.

[11] G. Smith, Writer, *Wavelength Dispersive X-Ray Fluorescence Course 18th-19th May 2017.* [Performance]. Scientific and Medical Products Ltd, 2017.

[12] Bruker, Writer, *Physics of X-Rays.* [Performance].

[13] M. Bounakhla and M. Thari, Writers, *X-ray Fluorescence Analytical Techniques.* [Performance]. CNESTEN.

[14] Bruker, Introduction to X-ray Fluorescence Analysis, Karlsruhe: Bruker, 2004.

[15] K. Mauser, Writer, *XRF-Basics.* [Performance]. Bruker.

[16] Rigaku, "Tube-above wavelength dispersive X-ray fluorescence spectrometer," January 2018. [Online]. Available: https://www.rigaku.com/en/products/xrf/primus2. [Accessed 19 January 2018].

[17] Bruker, Writer, *Instrument Parameters.* [Performance].

[18] Rigaku, "ZSX Primus Series Instruction Chapter 4.".

[19] Fluxana, "Fluxana XRF Application Solutions," 2017. [Online]. Available: https://www.fluxana.com/reference-material/drift-monitor. [Accessed 26 December 2017].

[20] M. Banzhaf, Writer, *XRF-Webinar.* [Performance]. Neste, 2016.

[21] R. S. FluXana, X-Ray Fluorescence Analysis: Practical and Easy, Bedburg-Hau, 2016.
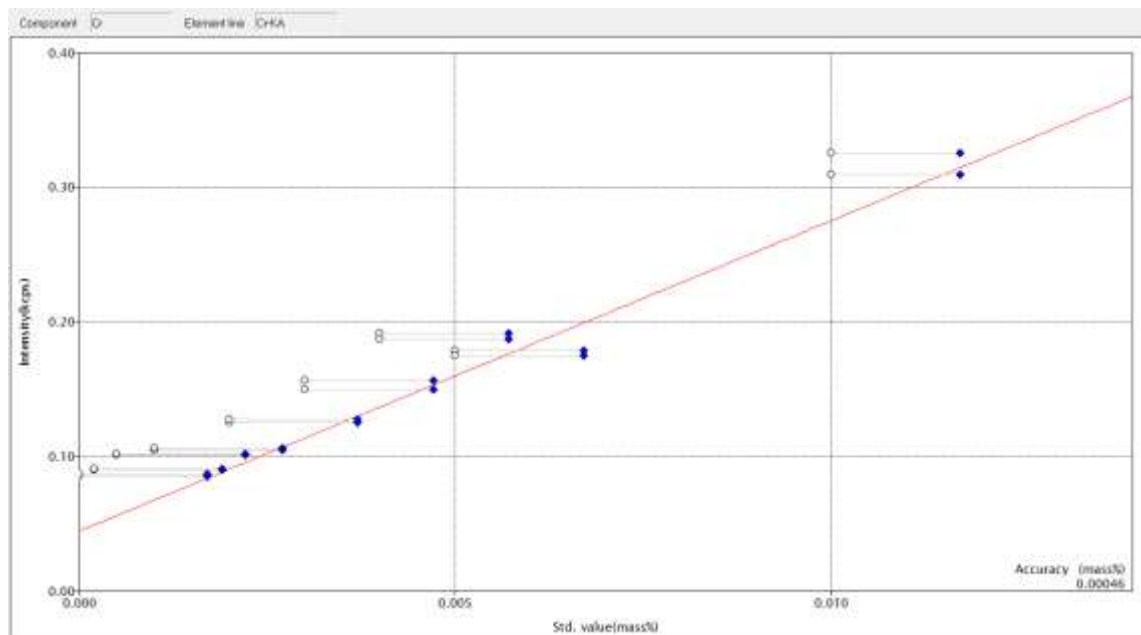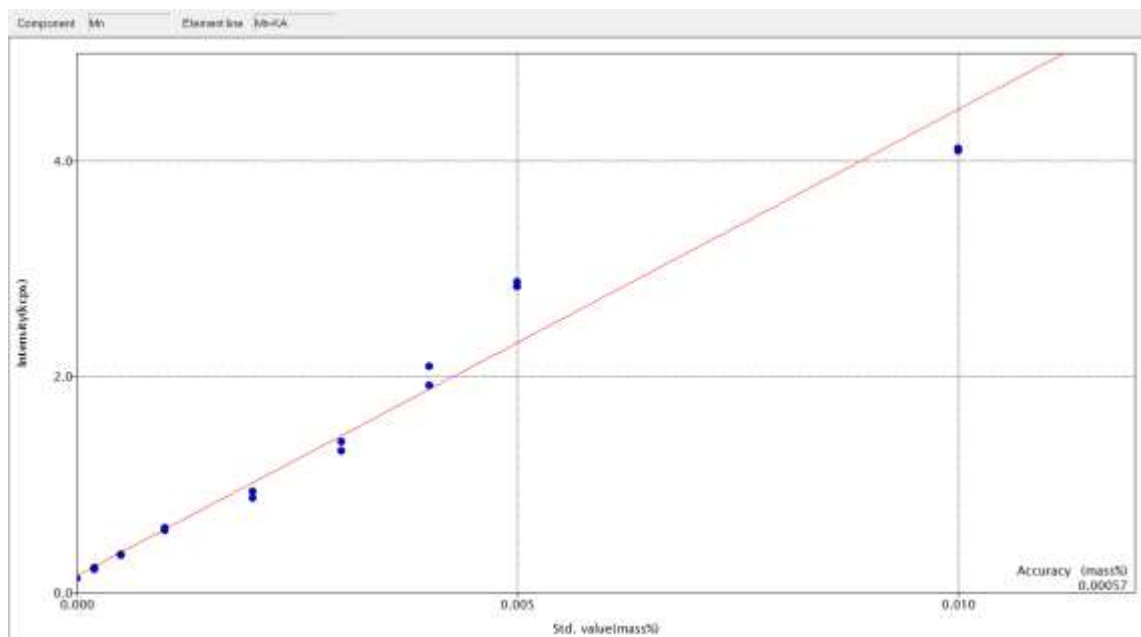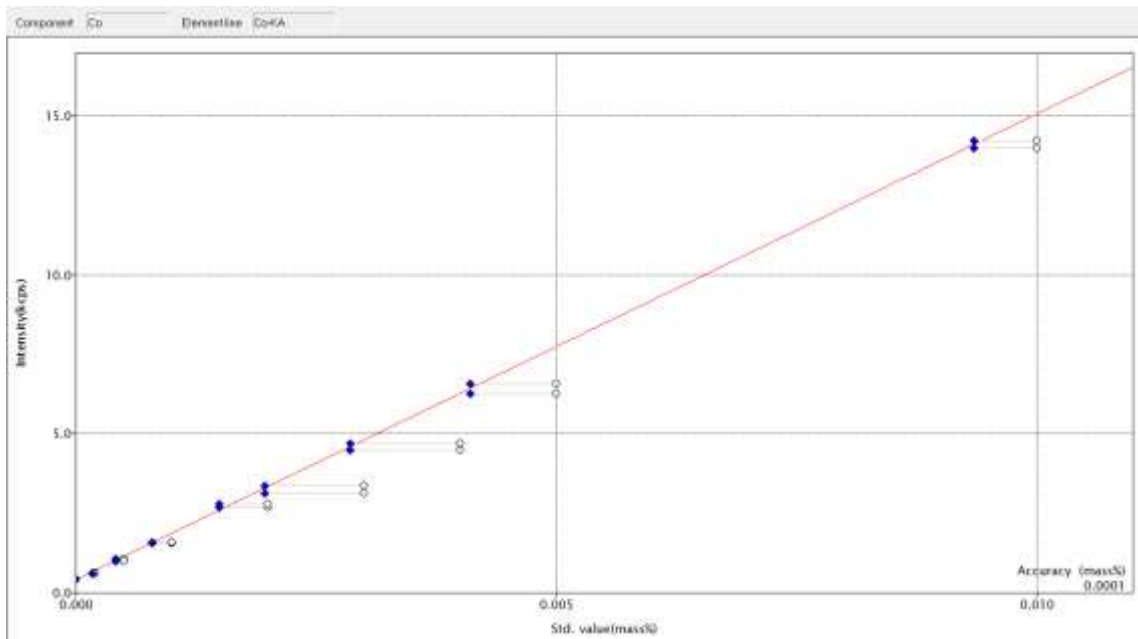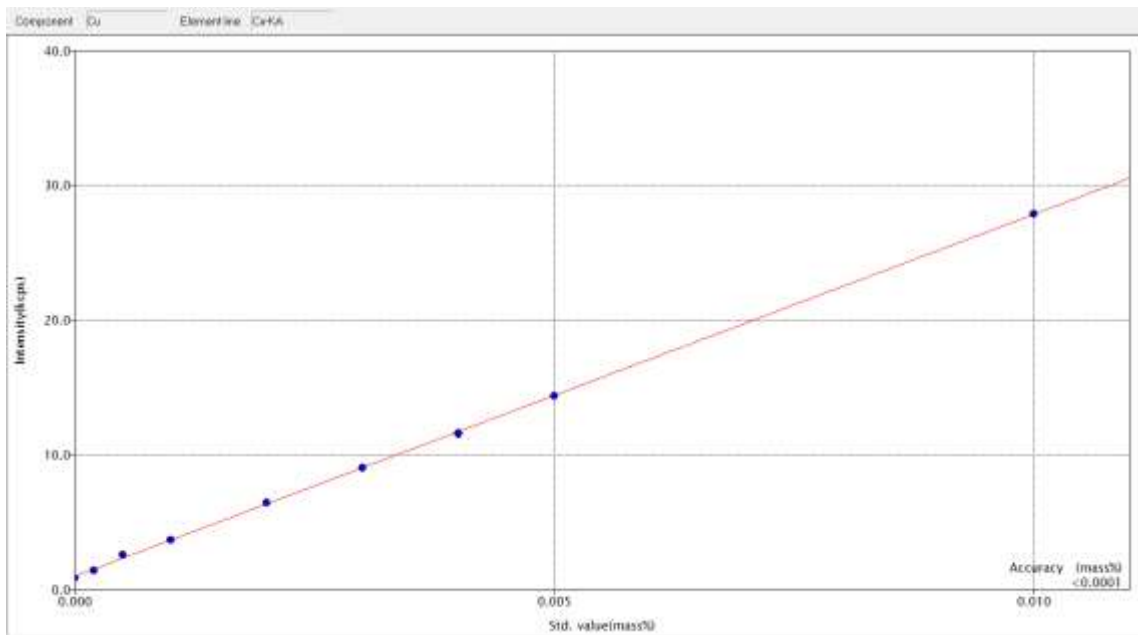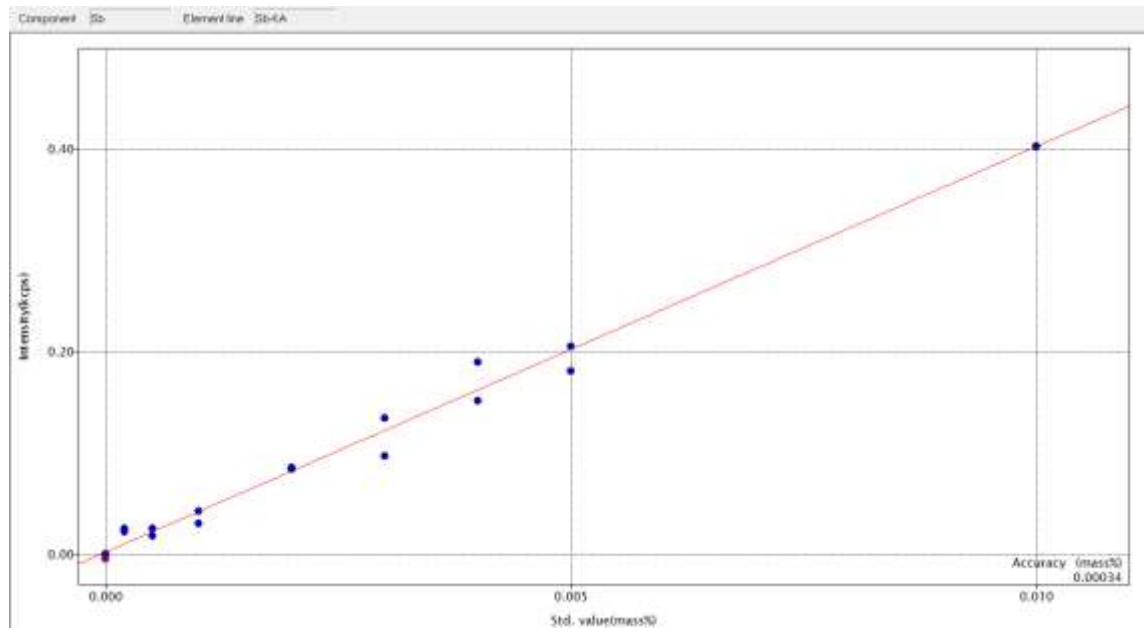
Calibration Curves

K-KA
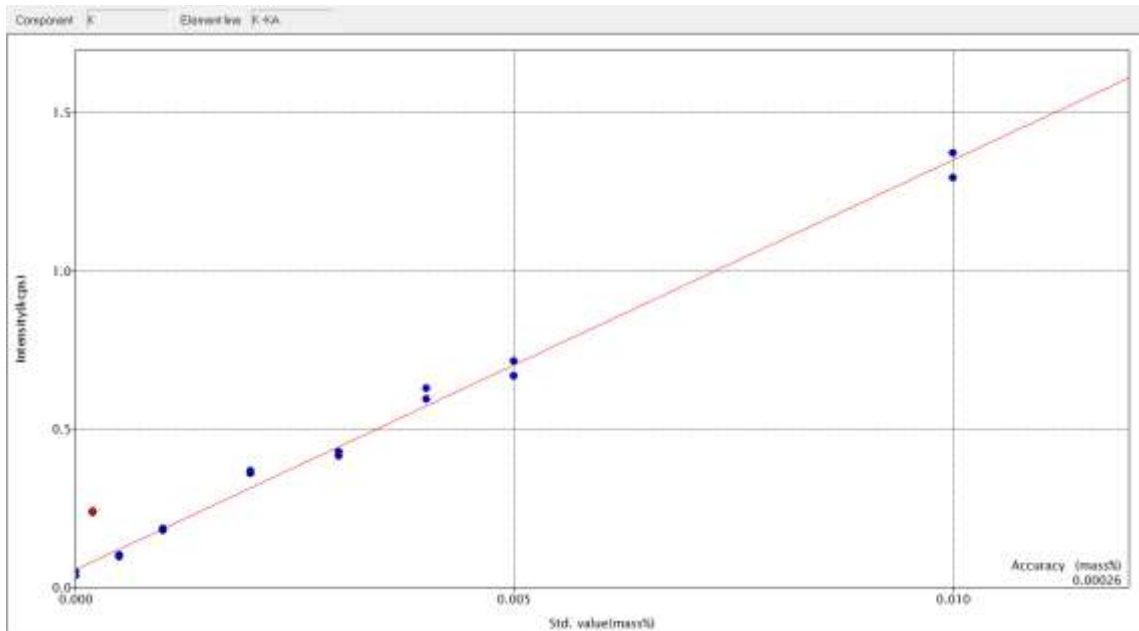
Ca-KA
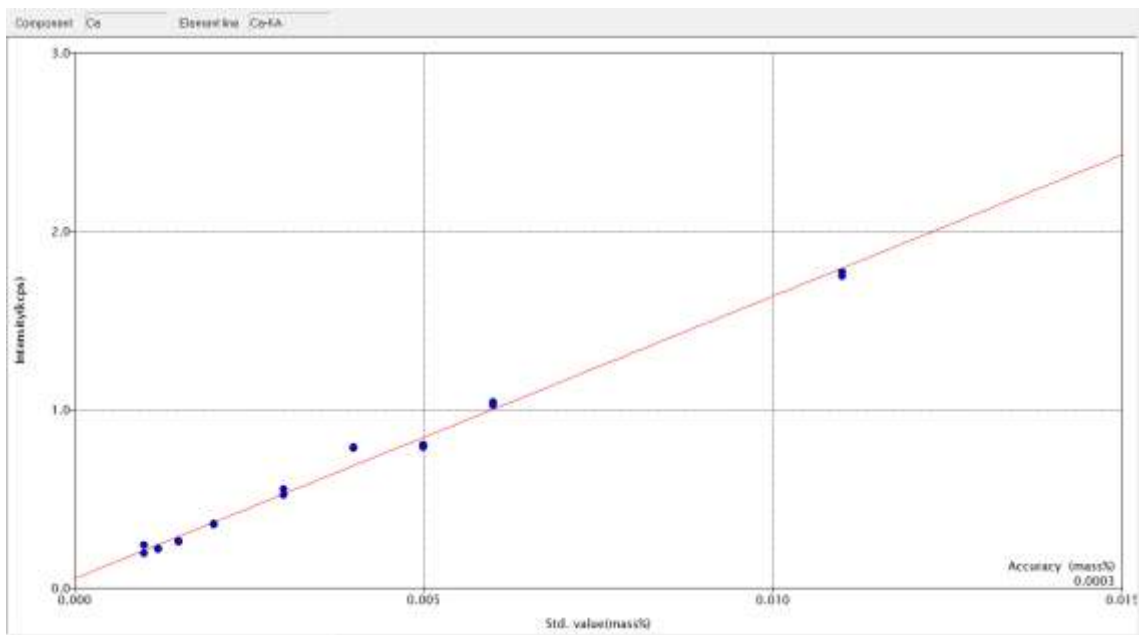
Cr-KA

Mn-KA

Co-KA

Cu-KA

Zn-KA

Cd-KA

Sn-KA

Sb-KA

Tl-LA

Pb-LA